

1 Alkalinity sources in the Dutch Wadden Sea

2 Mona Norbistrath^{1,2,3}, Justus E. E. van Beusekom¹, & Helmuth Thomas^{1,2}

3 ¹Institute of Carbon Cycles, Helmholtz-Zentrum Hereon, Geesthacht, 21502, Germany

4 ²Institute for Chemistry and Biology of the Marine Environment (ICBM), Carl von Ossietzky University Oldenburg,
5 Oldenburg, 26129, Germany

6 ³now at: Department of Marine Chemistry and Geochemistry, Woods Hole Oceanographic Institution, Woods Hole, MA,
7 02543, USA

8 *Correspondence to:* Mona Norbistrath (mona.norbistrath@gmail.com)

9 Abstract

10 Total alkalinity (TA) is an important chemical property playing a decisive role in the oceanic buffering capacity of CO₂. TA
11 is mainly generated by weathering on land, and by various anaerobic metabolic processes in water and sediments. The Wadden
12 Sea, located in the southern North Sea is hypothesized to be a source of TA for the North Sea, but quantifications are scarce.
13 This study shows observations of TA, dissolved inorganic carbon (DIC), and nutrients in the Dutch Wadden Sea in May 2019.
14 Along several transects, surface samples were taken to investigate spatial distribution patterns and to compare them with data
15 from the late 1980s. A tidal cycle was sampled to further shed light on TA generation and potential TA sources. We identified
16 the Dutch Wadden Sea as a source of TA and estimated an export of 6.6 Mmol TA per tide to the North Sea. TA was generated
17 in the sediments with deep pore water flow during low tide enriching the surface water. A combination of anaerobic processes
18 and CaCO₃ dissolution were potential TA sources in the sediments. We deduce that seasonality and the associated nitrate
19 availability in particular influence TA generation by denitrification, which is low in spring and summer.

20 1 Introduction

21 As the regulator of the ocean carbon dioxide (CO₂) sink, total alkalinity (TA) is of increasing scientific interest and is
22 investigated worldwide in the so called “Anthropocene” (Abril and Frankignoulle, 2001;Bozec et al., 2005;Chen and Wang,
23 1999;Dickson, 1981;Middelburg et al., 2020;Norbistrath et al., 2022;Renforth and Henderson, 2017;Thomas et al.,
24 2004;2009;Sabine et al., 2004). The “Anthropocene” describes the current era of our planet, when environmental changes,
25 driven by humans, have become identifiable in geological records (Zalasiewicz et al., 2010;Crutzen, 2002). One of the most
26 threatening changes for our climate is the anthropogenic driven increase in atmospheric greenhouse gases (GHG), such as
27 CO₂. To counteract the increasing atmospheric CO₂ concentrations and the ongoing climate warming, a combination of several
28 pathways is needed. Beside a strict reduction of CO₂ emissions, also net-negative emissions are required, which capture the
29 atmospheric CO₂ and store it either based on land or in the ocean (e.g., Keith et al., 2006;Matthews and Caldeira, 2008;Zhang

30 et al., 2022). The climate and the increasing atmospheric CO₂ content is also naturally regulated by the open ocean, and around
31 a quarter of the global anthropogenic CO₂ emissions are already removed by it (Friedlingstein et al., 2022). The carbon storage
32 capacity of the North Sea is an important atmospheric CO₂ sink as it exports the absorbed CO₂ in the deep layers of the Atlantic
33 Ocean where it is stored on longer time scales (Borges et al., 2005;Bozec et al., 2005;Burt et al., 2016;Brenner et al., 2016;Hu
34 and Cai, 2011;Schwichtenberg et al., 2020;Thomas et al., 2004;2009). Two important aspects of the oceanic climate regulation
35 are the oceanic circulation and TA. TA, primarily consisting of bicarbonate and carbonate, is generated by chemical rock
36 weathering (Suchet and Probst, 1993;Meybeck, 1987;Berner et al., 1983), and in various stoichiometries by calcium carbonate
37 (CaCO₃) dissolution and anaerobic metabolic processes, such as denitrification, which is the reduction process of nitrate to
38 dinitrogen gas in the nitrogen cycle (Hu and Cai, 2011;Wolf-Gladrow et al., 2007;Chen and Wang, 1999;Brewer and Goldman,
39 1976). Since TA, CO₂ uptake and its export to the deep ocean are mainly disentangled in the open ocean, TA and the oceanic
40 circulation interact closely in highly active and shallow ocean areas such coastal zones and continental and marginal shelves.
41 In these shallow areas, TA is susceptible to changes due to various metabolic processes and the influence of adjacent zones
42 like rivers, estuaries, marshes, and tidal flats (e.g., Norbistrath et al., 2022;2023;Wang et al., 2016;Voynova et al., 2019). A
43 previous study by Norbistrath et al. (2022) showed that an enhanced riverine, metabolic alkalinity would lead to increasing
44 CO₂ absorption in the coastal zones of the North Sea, highlighting the need to further investigate TA regulation in adjacent
45 zones of coastal oceans.

46 Coastal zones, which are the direct interface between most, if not all, compartments of the Earth system (i.e., atmospheric,
47 terrestrial, aquatic, and oceanic) and human societies, appear particularly vulnerable to environmental and climate change
48 (Glavovic et al., 2015). This holds true for the Wadden Sea, the shallow, coastal sea along an approximately 500 km coastline
49 of the Netherlands, Germany, and Denmark, in the southern North Sea, which is declared as an UNESCO world natural heritage
50 site since 2009. Most of the Wadden Sea is located between the protecting barrier Islands and the Mainland, which makes it
51 the world's largest uninterrupted stretch of tidal flats with multiple tidal inlets (Fig. 1). Due to the topography, the Wadden
52 Sea is a highly dynamic ecosystem with influences from the mainland and the North Sea (Hoppema, 1993;Postma, 1954;van
53 Raaphorst and van der Veer, 1990). Driving forces of the biogeochemical dynamics in the Wadden Sea are nutrient imports
54 by rivers and high suspended particulate matter (SPM) and organic matter (OM) imports from the North Sea (van Beusekom
55 et al., 2019;van Beusekom et al., 2012;Postma, 1954). Physical sources of variability in the Wadden Sea are oceanic driven
56 wind, waves, and tidal currents, as well as the counterclockwise circulation of the North Sea (Elias et al., 2012). Large tidal
57 amplitude and currents in conjunction with shallow water depths allow for vertical water column mixing and an exchange
58 between the pelagic and benthic realms including deep pore water exchange (Røy et al., 2008). The strong tidal currents also
59 impact the biogeochemistry of the North Sea (Postma, 1954), as they cause an exchange of water between the North Sea and
60 the Wadden Sea and play an important role in the import of particulate matter from the North Sea (Burchard et al., 2008).
61 Previous studies identified the Wadden Sea as a TA source for the North Sea with a loading between 39 Gmol yr⁻¹
62 (Schwichtenberg et al., 2020) and 73 Gmol yr⁻¹ (Thomas et al., 2009). Both studies suggested the entire Wadden Sea as one of
63 the most important TA sources of the carbon storage capacity for the North Sea. Burt et al. (2016) highlighted the importance

64 of coastal TA production for regulating the buffer system in the North Sea, and suggested denitrification as the major TA
65 source. Due to the strong connection between the North Sea and the Wadden Sea, a better understanding of TA generation in
66 the latter is required. Here, we focus on the Dutch Wadden Sea that has been well-studied during the past decades (Hoppema,
67 1990, 1991, 1993;De Jonge et al., 1993;Elias et al., 2012;Ridderinkhof et al., 1990;Postma, 1954;van Beusekom et al.,
68 2019;Schwichtenberg et al., 2017). In particular Hoppema (1990);(1993) observed the spatial and temporal variability of TA
69 in May in the late 1980s, which we compare with our observed transect data to detect potential differences over the last 30
70 years. In addition, we further discussed potential TA sources in the Dutch Wadden Sea.

71 **2 Methods**

72 **2.1 Study site and sampling**

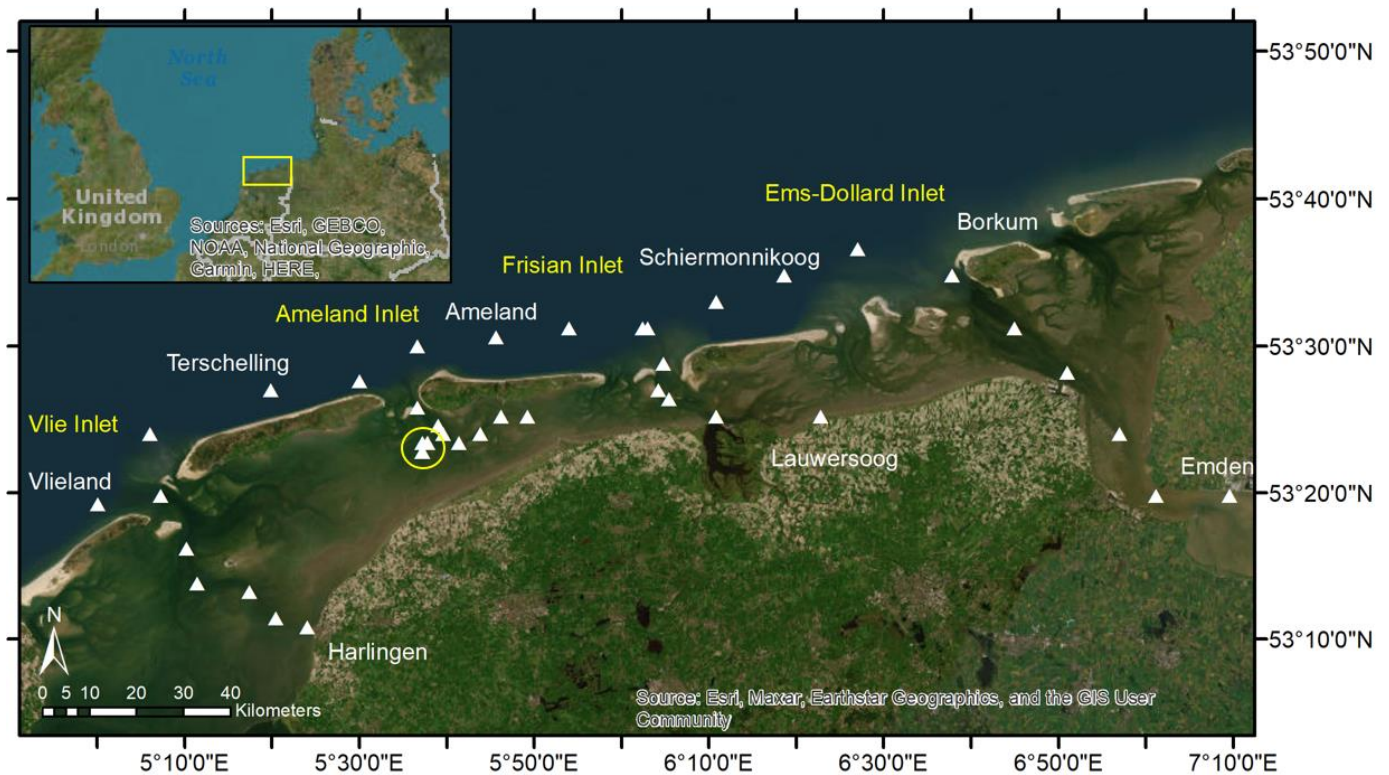
73 This study is based on samples collected on a research cruise (LP20190515) in the Dutch Wadden Sea (Frisian Islands) on RV
74 *Ludwig Prandtl* in May 2019 (Fig. 1). We collected water samples in the Wadden Sea starting at Harlingen, through the Vlie
75 Inlet along the islands Vlieland and Terschelling, through the Ameland Inlet to Ameland Island, from there on via the Frisian
76 Inlet to Lauwersoog, and around Schiermonnikoog Island via the Ems-Dollard Inlet to Emden. In addition, we sampled a half
77 tidal cycle during ebb tide (from high tide to low tide) on 21 May 2019. To set the range of ebb tide data in relation, we also
78 sampled a half tidal cycle during flood tide (from low tide to high tide) on 23 May 2019 for comparison. Both half tidal cycles
79 were sampled as an anchor station in the waterway at the western side of Ameland in the Ameland Inlet on each day.

80 Nearly half-hourly, we collected discrete surface (1.2 m depth) water samples with a bypass from the onboard flow-through
81 FerryBox system, which also provided essential physical parameters such as salinity with an accuracy of 0.02 (PSU) and
82 temperature with an accuracy of 0.1 °C (Petersen et al., 2011). The FerryBox was cleaned and the system checked prior to the
83 cruise, and salinity is occasionally checked using discrete samples, which is considered sufficient for gradients in near-shore
84 investigations (pers. comm. Y. Voynova). We complemented our salinity and temperature data with data from three
85 Rijkswaterstaat stations (Dantziggat, Terschelling 10, and Vliestroom; Table B3), which were close to our stations.

86 For TA and DIC measurements we sampled water with overflow into 300 mL BOD (biological oxygen demand) bottles and
87 preserved them with 300 µL saturated mercury chloride solution (HgCl₂) to stop biological activity. Each BOD bottle was
88 filled without air bubbles and closed by using a ground-glass stopper coated in Apiezon® type M grease and a plastic cap. The
89 samples were stored in a cool dark environment until measurements in the lab.

90 Water for nutrient samples was filtered through pre-combusted (4 h, 450 °C) GF/F filters and the filtrate was stored frozen in
91 three 15 mL Falcon tubes for triplicate measurements in the lab.

92 To determine the total carbon (C), organic carbon (C_{org}) and nitrogen (N) concentrations in SPM and associated C_{org}:N ratios,
93 we used pre-combusted (4 h, 450 °C) GF/F filters, which were dried after sampling at 50 °C to remove all humidity and were
94 stored frozen afterwards until measurement.



95
 96 **Figure 1** Sampling site in the Dutch Wadden Sea. The sampling stations around the Frisian Islands in May 2019 are visualized
 97 with white triangles. The yellow circle highlights the anchor stations for the tidal cycle sampling in the Ameland Inlet on two
 98 days. During the sampling day from low tide to high tide, we had two samples that we took slightly more western due to
 99 drifting. The island and city names are shown in white, the inlets in yellow. The tidal flats and sedimentary structures are well
 100 visible between the barrier islands and the mainland.

101 2.2 Carbon species analyses

102 The parallel analyses of TA and DIC were carried out in March 2020 by using the VINDTA 3C (Versatile INSTRument for the
 103 Determination of Total dissolved inorganic carbon and Alkalinity, MARIANDA - marine analytics and data), which measures
 104 TA by potentiometric titration and DIC by coulometric titration both with a measurement precision $< 2 \mu\text{mol kg}^{-1}$ (Shadwick
 105 et al., 2011). Certified reference material (CRM batch # 187) provided by Andrew G. Dickson (Scripps Institution of
 106 Oceanography) was measured before and after the samples and used to ensure a consistent calibration of both measurements.
 107 The calcite and aragonite saturation states (Ω), the pH, and the seawater partial pressure of CO_2 ($p\text{CO}_2$) were computed with
 108 the CO_2SYS program (Lewis and Wallace, 1998), using the measured parameters TA and DIC, and salinity, temperature,
 109 silicate and phosphate as input variables, together with the dissociation constants from Mehrbach et al. (1973), as refit by
 110 Dickson and Millero (1987). Reported calculation uncertainties are ± 0.0062 for pH (Millero et al., 1993), $\pm 4.9 \%$ for the
 111 aragonite saturation state and $\pm 3.5 \%$ for $p\text{CO}_2$ (Orr et al., 2018).

112 **2.3 Nutrient analyses**

113 The nutrients were measured with a continuous flow automated nutrient analyzer (AA3, SEAL Analytical) and a standard
114 colorimetric technique (Hansen and Koroleff, 2007) for nitrate (NO_3^-), nitrite (NO_2^-), phosphate (PO_4^{3-}), and silicate (Si), and
115 a fluorometric method (K  rouel and Aminot, 1997) for ammonium (NH_4^+) (Grasshoff et al., 2009). The nutrient samples were
116 measured against Eurofins reference materials VKI SW4.1B (for NO_x , NO_2 and NH_4) and VKI SW4.2B (for Si and PO_4) in
117 July 2019. The maximum standard deviations were $0.322 \mu\text{mol L}^{-1}$ for NO_3^- , $0.014 \mu\text{mol L}^{-1}$ for NO_2^- , $0.081 \mu\text{mol L}^{-1}$ for
118 NH_4^+ , $0.014 \mu\text{mol L}^{-1}$ for PO_4^{3-} and $0.165 \mu\text{mol L}^{-1}$ for Si.

119 For the C_{org} determination, filters were acidified with 1N HCl and dried overnight to remove all inorganic carbon content.
120 Filters were measured with a CHN-elemental analyzer (Eurovector EA 3000, HEKAtech GmbH) in the Institute of Geology,
121 University Hamburg, and calibrated against a certified acetanilide standard (IVA Analysentechnik, Germany). The standard
122 deviations were 0.05 % for carbon and 0.005 % for nitrogen.

123 **2.4 Data analyses**

124 The data analyses were performed by using RStudio Version 1.3.1073    2009-2020 RStudio, PBC. The linear regression
125 Model II was performed by using the “lmodel2” R package, and the plots were created with the “ggplot2” R package.

126 **3 Results**

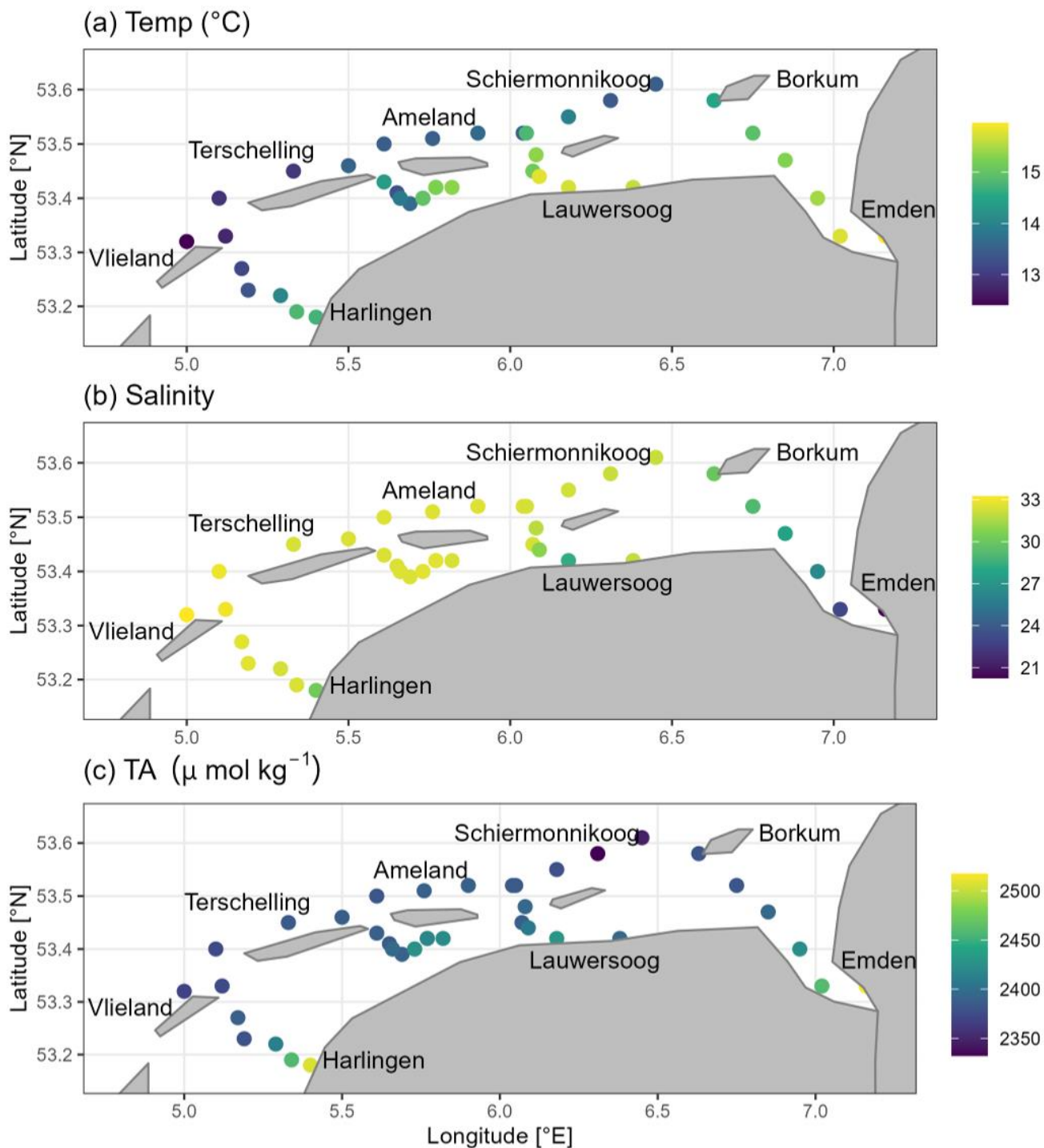
127 **3.1 Spatial parameter distribution**

128 To investigate the spatial distribution of TA in the Dutch Wadden Sea and compare its general status with earlier studies (in
129 particular Hoppema, 1990), we observed TA and related parameters in surface water along a transect from the coastal mainland
130 towards the North Sea.

131 The temperatures varied between 12 and 16   C with higher temperatures towards the coastal mainland (Fig. 2a). We identified
132 two main sub regions based on the salinity values. First the Ems-Dollard Inlet, which showed salinities lower than 28 and with
133 the minimum value of 20.25 at the most upstream station. And second, around Ameland Island and the remaining of our
134 investigated region in the Dutch Wadden Sea with salinities showing only smaller variations varying from 28 to 33 (Fig. 2b).
135 Spatial transect TA concentrations ranged from $2332 \mu\text{mol TA kg}^{-1}$ to $2517 \mu\text{mol TA kg}^{-1}$. We observed lower concentrations
136 on the North Sea side of the Frisian Islands with somewhat higher concentrations around Ameland (Fig. 2c). In contrast to the
137 North Sea side, the values were higher ($> 2380 \mu\text{mol TA kg}^{-1}$) in the Wadden Sea. In the Ems-Dollard Inlet, the concentrations
138 were even higher, with values up to $2517 \mu\text{mol TA kg}^{-1}$ at the most upstream station.

139 Silicate (Si) showed higher concentrations in the Wadden Sea and lower ones towards the North Sea (Fig. A1a). Highest
140 concentrations were observed at the coastal mainland and in the Ems-Dollard Inlet. Silicate concentrations ranged between 0.3
141 and $56.3 \mu\text{mol Si L}^{-1}$. Both, the calcite and aragonite saturation states (Ω) were supersaturated in the entire study region.

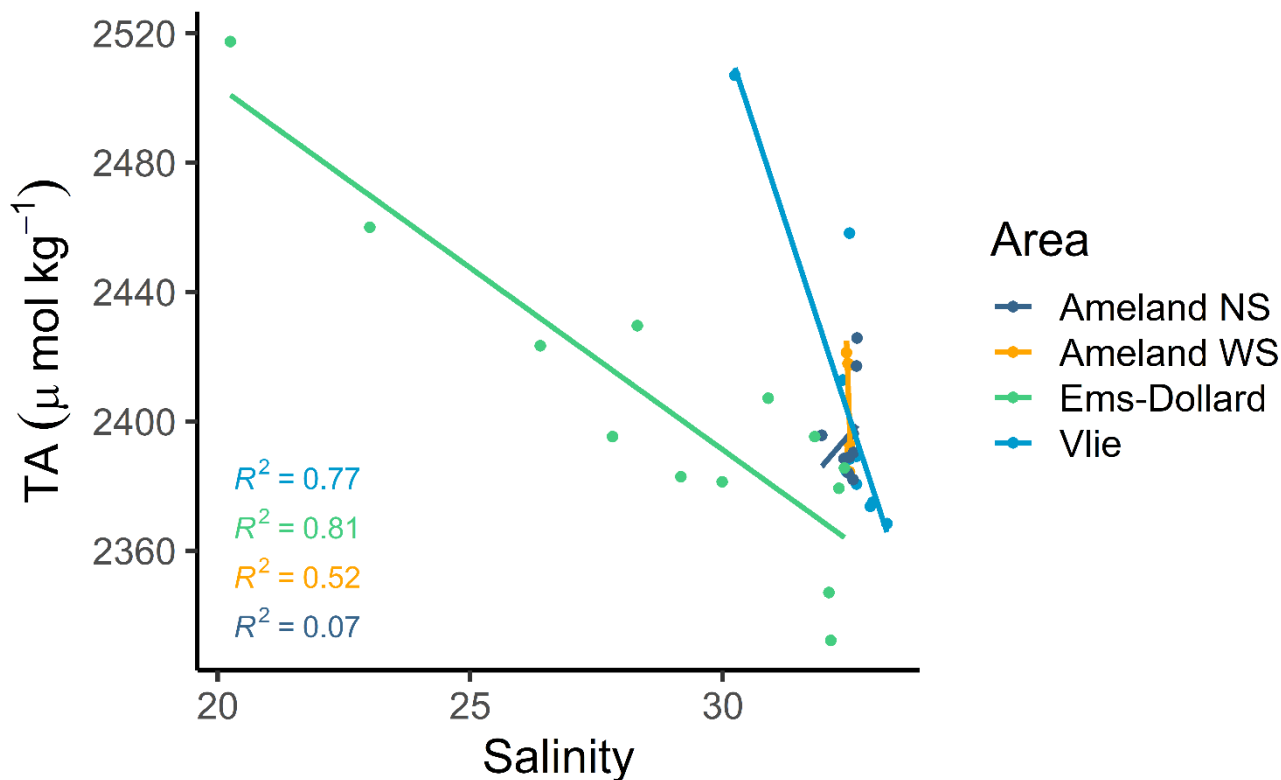
142 Saturation state values ranged from 2.3 to 4.6 for calcite (Fig. A1b), and from 1.4 to 2.8 for aragonite (Table B3). Highest
143 values were observed at the North Sea side of the barrier islands, and lowest values near Harlingen and in the Ems-Dollard
144 Inlet. Like the calcite and aragonite saturation states, the pH values were higher in the North Sea, and lower in the Wadden
145 Sea and near the coastal mainland (Fig. A1c). The pH values ranged from 7.86 to 8.19, and lowest values were observed near
146 Harlingen and in the Ems-Dollard Inlet. The nitrate (NO_3^-) concentrations were in a low range ($< 3 \mu\text{mol NO}_3^- \text{ L}^{-1}$) throughout
147 the study region. Higher concentrations ($< 6 \mu\text{mol NO}_3^- \text{ L}^{-1}$) were observed only at a few stations close to land, and maximum
148 concentrations ($< 38 \mu\text{mol NO}_3^- \text{ L}^{-1}$) were observed in the Ems-Dollard Inlet (Fig. A1d). DIC concentrations ranged from 2097
149 $\mu\text{mol DIC kg}^{-1}$ to 2430 $\mu\text{mol DIC kg}^{-1}$ (Fig. A1e). DIC values showed a similar pattern as TA values, with higher concentrations
150 near the coastal mainland and in the Ems-Dollard Inlet, and decreasing concentrations toward the North Sea, where DIC
151 reached minimum values.



152

153 **Figure 2** Spatial distribution of a) temperature ($^{\circ}\text{C}$), b) salinity (PSU), and c) total alkalinity (TA; $\mu\text{mol kg}^{-1}$) from surface
 154 water samples in May 2019.

155 Compared to the other transects of this study region, the strong influence of the inner Ems Estuary is visible at the most
156 upstream station in the Ems-Dollard Inlet, showing lowest salinity, lowest pH and calcite saturation state values, and highest
157 values of TA, DIC, nitrate, silicate and phosphate. The outer side of the Vlie Inlet reflects the North Sea conditions with lower
158 temperatures and higher salinities. The North Sea impact is also visible in the mixing plot between TA and salinity (Fig.
159 3). Statistical significant linear mixing behavior was observed in the transect through the Ems-Dollard Inlet ($R^2 = 0.81$) and
160 through the Vlie Inlet ($R^2 = 0.77$), where TA concentrations decreased with increasing salinities from the mainland towards
161 the North Sea (Fig. 3). Whereas in the Ems-Dollard Inlet mixing is dominated by riverine water with high TA concentrations,
162 the mixing in the Vlie Inlet showed a more prominent mixing of Wadden Sea and North Sea water. The TA concentrations in
163 the Vlie Inlet and around Ameland, both at the North Sea side (Ameland NS) and the Wadden Sea side (Ameland WS) were
164 higher than the TA concentration computed for the salinity end-member in the Ems-Dollard Inlet, suggesting the Dutch
165 Wadden Sea as a source of TA (Fig. 3). Both the Ameland NS and WS data clearly indicated a non-conservative behavior with
166 a range of TA concentrations at near constant salinities.



167

168 **Figure 3** Mixing plot of total alkalinity (TA) and salinity (PSU) in the North Sea side of Ameland and the Frisian Inlet
169 (Ameland NS), in the Wadden Sea site of Ameland (Ameland WS), around Schiermonnikoog and in the Ems-Dollard Inlet
170 (Ems-Dollard), and in the Vlie Inlet (Vlie).

171 **3.2 Tidal cycle**

172 We observed a half tidal cycle at an anchor station in the Ameland Inlet during ebb tide, to 1) identify potential TA sources
173 and 2) to quantify potential TA export to the North Sea. We identified patterns in several biogeochemical parameters in water
174 leaving the tidal flats (Fig. 4, Table B1). Temperature increased from 13.25 to 14.7 °C (Fig. 4a). Salinity was constant around
175 32.5 (Fig. 4b), which is in the range of coastal southern North Sea water excluding admixture of local fresh water sources.

176 During ebb tide, TA ranged from 2387 $\mu\text{mol TA kg}^{-1}$ during high tide to 2438 $\mu\text{mol TA kg}^{-1}$ during low tide (Fig. 4c). We
177 observed an increase of 51.6 $\mu\text{mol TA kg}^{-1}$ (ΔTA) during ebb tide (6.8 h), resulting in a TA increase of 7.6 $\mu\text{mol TA kg}^{-1} \text{ h}^{-1}$
178 at the sampling location.

179 DIC concentrations behaved similar to TA with minimum values at high tide (2172 $\mu\text{mol DIC kg}^{-1}$), and maximum values
180 (2273 $\mu\text{mol DIC kg}^{-1}$) at low tide, resulting in an increase of 101.3 $\mu\text{mol DIC kg}^{-1}$ (ΔDIC) or 14.9 $\mu\text{mol DIC kg}^{-1} \text{ h}^{-1}$ (Fig. 4d).
181 DIC increased almost twice as much as TA.

182 Nitrate increased during ebb tide by 0.92 $\mu\text{mol NO}_3^- \text{ L}^{-1}$ (ΔNO_3^-) from a minimum of 1.26 $\mu\text{mol NO}_3^- \text{ L}^{-1}$ to a maximum of
183 2.17 $\mu\text{mol NO}_3^- \text{ L}^{-1}$ (Fig. 4e), resulting in a nitrate increase of 0.13 $\mu\text{mol NO}_3^- \text{ L}^{-1} \text{ h}^{-1}$.

184 Silicate showed a similar pattern with low values (1.8 $\mu\text{mol Si L}^{-1}$) at high tide increasing during ebb tide to a maximum of
185 11.2 $\mu\text{mol Si L}^{-1}$, resulting in a silicate increase (ΔSi) of 9.4 $\mu\text{mol Si L}^{-1}$ or 1.4 $\mu\text{mol Si L}^{-1} \text{ h}^{-1}$ during ebb tide (Fig. 4f).

186 Ammonium increased from 3.47 $\mu\text{mol NH}_4^+ \text{ L}^{-1}$ to 6.22 $\mu\text{mol NH}_4^+ \text{ L}^{-1}$ during ebb tide (Fig. 4g), resulting in an ammonium
187 increase (ΔNH_4^+) of 2.74 $\mu\text{mol NH}_4^+ \text{ L}^{-1}$, or 0.4 $\mu\text{mol NH}_4^+ \text{ L}^{-1} \text{ h}^{-1}$.

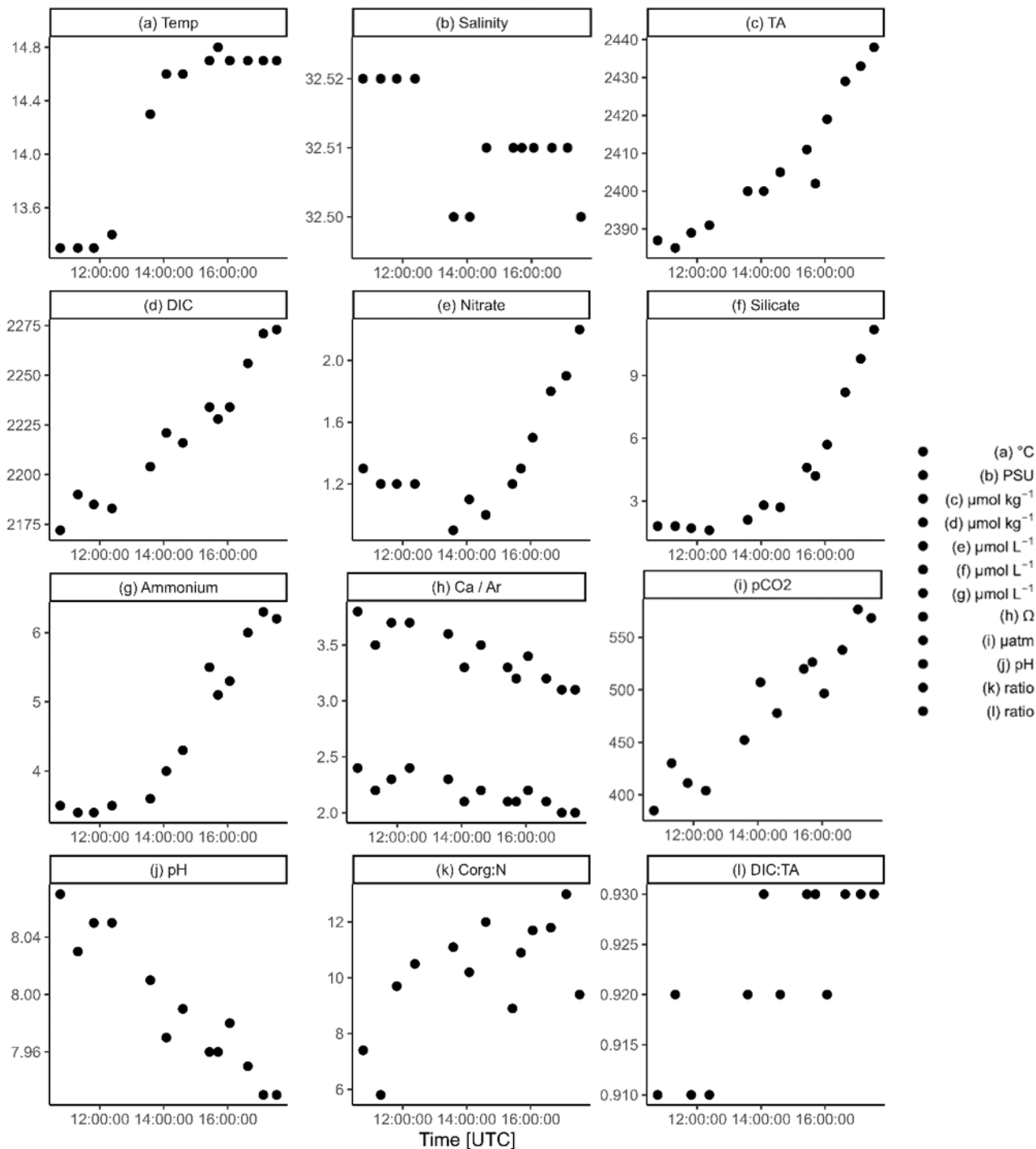
188 The calcite and aragonite saturation states had maximum values ($\Omega_{\text{Ca}} = 3.8$, $\Omega_{\text{Ar}} = 2.4$) at high tide and decreased to their
189 minimum ($\Omega_{\text{Ca}} = 3.1$, $\Omega_{\text{Ar}} = 2.0$) during ebb tide (Fig. 4h). The influence of the North Sea is indicated by the observed maximum
190 at high tide, which decreased during the ebb.

191 The seawater $p\text{CO}_2$ had minimum values at high tide (385.1 μatm) and increased up to 576.6 μatm during low tide (Fig. 4i).

192 Like Ω , the maximum pH was 8.07 at high tide and decreased to a minimum (7.93) during ebb tide (Fig. 4j).

193 $\text{C}_{\text{org}}:\text{N}$ ratios of SPM increased during ebb tide (Fig. 4k). A minimum $\text{C}_{\text{org}}:\text{N}$ ratio of 5.6 was observed around high tide and
194 increased to a maximum of 13.0 during ebb tide. Simultaneously, the SPM concentration increased during ebb tide, from 12.8
195 mg SPM L^{-1} to a maximum of 82.4 mg SPM L^{-1} at the second last station (Table B1).

196



197

198 **Figure 4** A half tidal cycle from high tide to low tide. Temporal distribution of a) temperature, b) salinity, c) total alkalinity
 199 (TA), d) dissolved inorganic carbon (DIC), e) nitrate, f) silicate, g) ammonium, h) calcite (upper points) and aragonite (lower

200 points) saturation states (Ω), i) $p\text{CO}_2$ (μatm), j) pH, k) $\text{C}_{\text{org}}:\text{N}$ ratio of SPM, and l) DIC:TA ratio. Note the different y-axes
201 and the +1 hour time difference between the local time and the UTC time.

202 3.3 TA generation

203 Tidal forcing leads to a bi-diurnal exchange between Wadden Sea and North Sea water. The tidal forcing also induces a strong
204 benthic-pelagic coupling (Huettel et al., 2003; Røy et al., 2008). Many studies support that the outflowing water exports
205 material from the sediment including remineralization products from organic matter (e.g., Billerbeck et al., 2006; Røy et al.,
206 2008). Here, we focus on the hypothesis that the sediments are a significant source of TA.

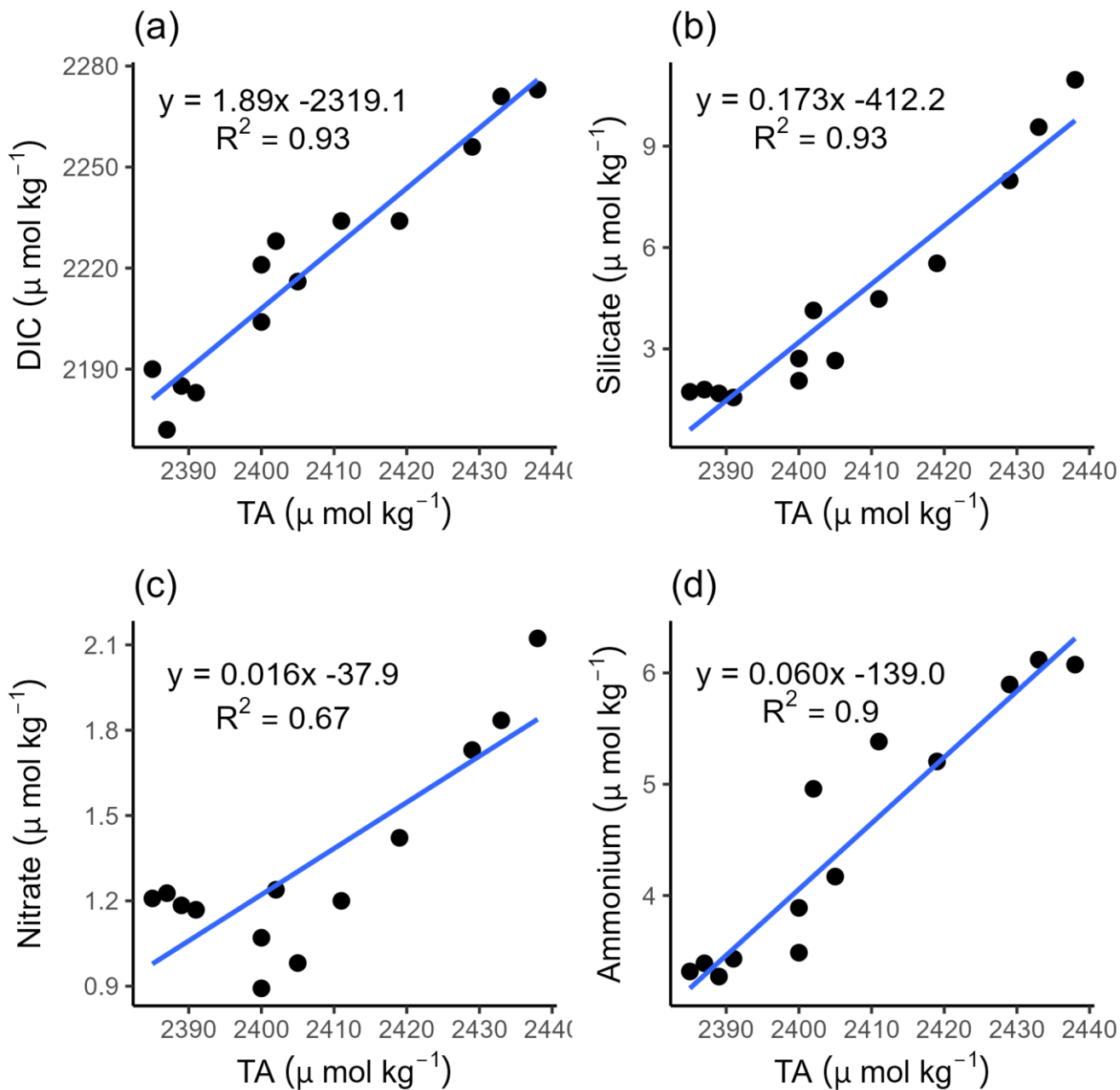
207 For a first rough estimate of a maximum TA export during ebb tide, we used the mean observed TA increase ($\Delta\text{TA} / 2$) of 25.8
208 $\mu\text{mol TA kg}^{-1}$ during ebb tide (in the Ameland Inlet, part of the Borndiep tidal basin), a tidal prism of $478 \cdot 10^6 \text{ m}^3$ of the
209 Borndiep tidal basin, and a share of intertidal flats of 53 % (Louters and Gerritsen, 1994). Assuming that only the intertidal
210 sediments exchange TA, we estimated a TA export of 6.6 Mmol TA per tide to the North Sea. Assuming two ebb tides and a
211 lunar cycle of 24.8 hours this would result in a daily export of 12.7 Mmol TA.

212 The significant correlation of TA and silicate ($R^2 = 0.93$), and the insignificant relation between TA and salinity ($R^2 = 0.32$),
213 as well as silicate and salinity ($R^2 = 0.21$), suggest that TA originates from the tidal flats in this part of the Dutch Wadden Sea
214 and is not from admixture carried by river runoff. The significant correlation between TA and silicate both during ebb tide
215 point to the same source (Fig. 5b).

216

217 To further elucidate potential TA sources in the Dutch Wadden Sea, we correlated TA with DIC, silicate, nitrate, and
218 ammonium in the half tidal cycle from high tide to low tide, respectively (Fig. 5).

219 The correlation between TA and DIC is a measure between anaerobic and aerobic processes. Our data show a strong positive
220 correlation between DIC and TA ($R^2 = 0.93$) with TA concentrations being higher than DIC concentrations (Fig. 5a). We
221 observed a release excess of DIC compared to TA as indicated by the slope of 1.89 and by an increase in DIC ($\Delta\text{DIC} = 101.3$
222 $\mu\text{mol kg}^{-1}$) almost twice as high as TA ($\Delta\text{TA} = 51.6 \mu\text{mol kg}^{-1}$) (Fig. 5a). This excess DIC may be caused by strong CO_2
223 production due to high aerobic OM degradation, which can be supported by seawater being supersaturated in $p\text{CO}_2$ with respect
224 to the atmosphere (Fig. 4i). The TA increase can be fueled by various processes which we will discuss below. We detected a
225 linear positive correlation of increasing TA and silicate ($R^2 = 0.93$) during ebb tide, supporting pore water outflow (Fig. 5b)
226 as pore water is the major Si source during summer (van Bennekom et al., 1974). A stronger influence of the pore water with
227 ongoing ebb tide is indicated by increasing values. The positive correlation between nitrate and TA ($R^2 = 0.67$) (Fig. 5c) was
228 less strong than the correlations between TA and DIC, and TA and Si, which could be traced back to an effect of the first four
229 sampling points that were probably at the tipping point from high tide to low tide. In the remaining samples, the increasing
230 nitrate and TA concentrations suggest a stronger TA generation than nitrate production, balancing TA that may be consumed
231 by nitrification (i.e., nitrate production).



232

233 **Figure 5** Correlations of TA with a) dissolved inorganic carbon (DIC), b) silicate, c) nitrate, and d) ammonium during ebb

234 tide in the Ameland Inlet.

235 4 Discussion

236 4.1 Spatial TA variability

237 Hoppema (1990) reported TA distributions in the westernmost part of the Dutch Wadden Sea around the barrier islands Texel,
238 Vlieland, and Terschelling. He focused on the tidal basins drained by the tidal inlets Marsdiep and Vlie located more to the
239 west than our sampling stations (not visible on the map). Hoppema (1990) did not observe a continuous increase of salinity in
240 the Wadden Sea from the fresh water source towards the North Sea and associated this to the influence of tidal differences and
241 an arbitrary sampling scheme. The presence (dominance) of North Sea water in the Dutch Wadden Sea and on the tidal flats
242 is supported by our transect data, which show relatively high salinities at coastal North Sea level. Brackish salinities were only
243 detected in the Ems-Dollard Inlet, which receives fresh water from the river Ems, and close to Harlingen and Lauwersoog,
244 which have direct fresh water inflows by smaller rivers and streams. The absence of clear salinity gradients in the more eastern
245 part of the Dutch Wadden Sea investigated in our study suggest that most of the IJsselmeer discharge was exchanged with the
246 North Sea through the Marsdiep (e.g., Duran-Matute et al., 2014).

247

248 The spatial TA data by Hoppema (1990), show lower TA concentrations at stations with more fresh water influence and higher
249 TA concentrations in the tidal inlets. The data of this study also show high TA concentrations in the tidal inlets, suggesting
250 TA generation in sediments, which is possibly fueled by high imports of nutrients and OM (van Beusekom and De Jonge,
251 2002). The even higher TA concentrations at stations with lower salinities close to the mainland observed in this study also
252 show the influence from the catchment area on the coast, and possibly TA generation in the shallow sediments near the coast.
253 In May 1986, Hoppema (1990) found TA concentrations ranging between 2319 and 2444 $\mu\text{mol TA kg}^{-1}$ at salinities between
254 18.62 and 29.17. Our lowest observed TA concentration was 2332 $\mu\text{mol TA kg}^{-1}$ at a salinity of 32.14, and our highest TA
255 concentration was 2517 $\mu\text{mol TA kg}^{-1}$ at a salinity of 20.25 close to the coastal mainland. A comparison of both studies shows
256 that the general TA levels are in a similar range, but that the spatial gradients are opposite.

257 A conservative mixing between TA and salinity is only visible in the Ems-Dollard Inlet and the Vlie Inlet (Fig. 3). While the
258 conservative mixing in the Ems-Dollard Inlet is more dominated by the fresh water discharge from the Ems River, the
259 conservative mixing in the Vlie Inlet is more dominated by North Sea water passing through this deep inlet and allowing more
260 North Sea water to be transported towards the coast. After the Marsdiep Inlet, the Vlie Inlet has the highest average tidal prism
261 and is the second largest inlet in the Dutch Wadden Sea (Elias et al., 2012). Similar to our findings, Hoppema (1990) noted a
262 linear mixing of TA and salinity in the Vlie Inlet, and suspected a lower fresh water contribution there as well, which is in
263 accordance with model data (Duran-Matute et al., 2014).

264 In the Ems-Dollard Inlet, conservative mixing was observed, indicating minor contributions from other sources. In a previous
265 study, Norbistrath et al. (2023) observed very high TA concentrations and TA generation in the upper tidal river of the highly
266 turbid Ems Estuary, which may explain the high levels of TA in the Ems-Dollard Inlet (at low salinities) observed in this study.

267 Hoppema (1990) also observed a range of TA concentrations in the Dutch Wadden Sea and related these to different sinks and
268 sources. TA sinks can be calcium carbonate (CaCO_3) precipitation, or extraction of seawater carbonate by mollusks (e.g., Chen
269 and Wang, 1999;Hoppema, 1990). Variable fresh water inflows can either serve as a sink or a source (e.g., Chen and Wang,
270 1999;Hoppema, 1990). Other TA sources can be CaCO_3 dissolution, anaerobic metabolic processes in the sediment, or erosion
271 of TA enhancing sediments (e.g., Hoppema, 1990;Chen and Wang, 1999).

272 Except for the Ems-Dollard Inlet and close to Harlingen, we observed mainly marine salinities (> 30) but higher TA values in
273 the Dutch Wadden Sea than in the North Sea. We therefore exclude possible TA sinks and focus only on TA sources. According
274 to Hoppema (1990), the main causes for TA variations in the Dutch Wadden Sea were fresh water inflows and sources in the
275 sediment. In our study, fresh water inflows with high TA concentrations were only observed in the Ems-Dollard Inlet, but not
276 around the islands and the tidal flats. For a further TA source identification in the Dutch Wadden Sea, we investigated the TA
277 variability during ebb tide in a tidal channel close to Ameland.

278 **4.2 Determination of TA generation**

279 Burt et al. (2016) and Schwichtenberg et al. (2020) indicated TA generation in the Wadden Sea as an important source for the
280 North Sea's carbon storage capacity. Here, we want to further identify TA generation and potential TA sources.

281 In a study from the late 1980s, Hoppema (1993) observed a tidal cycle in the Marsdiep in May and September. Focusing on
282 TA, DIC, and oxygen, he also observed increasing TA values during ebb tide and assumed the tidal flats and discharging rivers
283 and canals as TA sources. Comparing our present TA data and the historical TA data, there is not a large difference in the
284 range of values observed during a tidal cycle. However, a further in-depth interpretation and comparison of both TA data sets
285 is limited by the low number of data, leading us to focus on TA generation during our cruise.

286 We made a very rough first estimate of the daily TA export. By using a 3D ecosystem model, Schwichtenberg et al. (2020)
287 estimated an annual export of 10 to 14 Gmol TA yr^{-1} for the entire Dutch Wadden Sea. Given that the Borndiep tidal basin
288 covers about 14% of the Dutch Wadden Sea and assuming no seasonal dynamics, our estimate of 12.7 Mmol d^{-1} compares
289 well with the annual averaged model estimate of 4.6 Mmol TA d^{-1} , but the overestimation suggests that seasonal dynamics
290 may be involved. Since our TA export based only on a half tidal observation, the inclusion of it into the model used by
291 Schwichtenberg et al. (2020) would be unreliable (pers. comm. J. Pätsch, 2022). To test whether the observed TA generation
292 matches their suggested TA export, observational data of at least each season are required to run the model and gain a
293 representative result (pers. comm. J. Pätsch, 2022).

294 **4.3 TA source attribution**

295 **4.3.1 Local sediment outwash**

296 In order to gain further insight into potential sources of TA, we compared our TA and nutrient data. The main focus was on
297 dissolved silicate (Si) as van Bennekom et al. (1974) showed that this nutrient is depleted in the Wadden Sea during the spring

298 diatom blooms and further showed that pore water is the main source of dissolved Si during summer. It is important to note
299 that winter concentrations in the Rhine (main contributor to the IJsselmeer) have not changed much since the 1970s and
300 showing maximum concentrations of about $125 \mu\text{mol Si L}^{-1}$ in winter and clear seasonal dynamics due to uptake by diatoms
301 (unpublished results based on data provided by Pätsch (2024); available through [https://wiki.cen.uni-](https://wiki.cen.uni-hamburg.de/ifm/ECOHAM/DATA_RIVER)
302 [hamburg.de/ifm/ECOHAM/DATA_RIVER](https://wiki.cen.uni-hamburg.de/ifm/ECOHAM/DATA_RIVER)). We identified a silicate increase of $1.4 \mu\text{mol Si L}^{-1} \text{ h}^{-1}$ during ebb tide. Due to
303 the absence of large estuaries nearby and salinity consistently being above 32 at our tidal sampling station near the island of
304 Ameland, we exclude fresh water runoff as a major silicate source and indicate TA sources within the Wadden Sea.
305 Submarine groundwater discharge (SGD) was identified as a source for nutrient fluxes in tidal flat ecosystems in previous
306 studies (e.g., Billerbeck et al., 2006; Røy et al., 2008; Santos et al., 2021; Waska and Kim, 2011; Wu et al., 2013). Since we
307 observed relatively constant marine salinities, we suspect that deep pore water flow (e.g., Røy et al., 2008) enriched with
308 nutrients act as a source for our observed increasing TA and nutrients parameters. TA generation in tidal flats was also observed
309 by Faber et al. (2014), who focused on a large macro tidal embayment in southern Australia. They also found increasing TA
310 values during ebb tide, associated the TA increase with a higher fraction of pore water, and determined the tidal cycle as the
311 controlling force for pore water exchange. Their findings and the observed silicate outwash support our assumption that TA is
312 generated in the sediments of the tidal flats and is washed out during ebb tide. In addition, we exclude lateral advected signals
313 from more western regions as the Vlie Inlet, since the TA concentrations in the surface transect samples in the Vlie Inlet
314 (except of the two samples close to the coastal mainland near Harlingen) were in the same range as the other observed TA
315 concentrations and were smaller than the increasing TA concentrations during ebb tide. Both increases in TA and silicate are
316 tidal signals, and we identify TA generation in the sediments of the tidal flats here as the major local TA source.

317 **4.3.2 TA generating processes**

318 The deduced TA generation of $7.6 \mu\text{mol TA kg}^{-1} \text{ h}^{-1}$ and the silicate increase of $1.4 \mu\text{mol Si L}^{-1} \text{ h}^{-1}$ indicated an excess of TA
319 compared to silicate (also Fig. 5b). Considering a supposed TA:Si ratio of 2:1 (Marx et al. 2017), the observed $1.4 \mu\text{mol Si L}^{-1}$
320 h^{-1} would then account for a TA generation of $2.8 \mu\text{mol TA kg}^{-1} \text{ h}^{-1}$. High silicate concentrations in tidal flat pore water
321 (Rutgers van der Loeff, 1974) and in situ production of silicate from dissolving diatom frustules are the most probable sources
322 of the silicate (e.g., van Bennekom et al., 1974). Since we observed more TA generated than silicate being washed out, other
323 biogeochemical processes must be responsible for the TA generation in the sediments of the tidal flats in the Dutch Wadden
324 Sea.

325

326 We exclude CaCO_3 dissolution as TA source in the water column, since the Ω values were supersaturated with $\Omega > 1$ (Fig. 4h,
327 Table B1). The continuous calcite supersaturation nicely indicated the inflow and dominance of North Sea water during the
328 flood, with Ω values similar to previously observed North Sea values ($\Omega \sim 3.5$ to 4) (Charalampopoulou et al., 2011; Carter et
329 al., 2014). In pore water, carbonate undersaturation and associated CaCO_3 dissolution can only be driven metabolically, due

330 to CO₂ production by OM remineralization, or due to the reoxidation of compounds reduced previously by anaerobic processes
331 (Brenner et al., 2016;Jahnke et al., 1994).

332

333 Other potential sources of TA generation in the sediments can be further narrowed down by a more detailed interpretation of
334 changes in DIC (Δ DIC) and TA (Δ TA) during ebb tide, and their combination with various nutrient ratios. The correlation of
335 DIC and TA reveals an increase in DIC (Δ DIC) almost twice as high as in TA (Δ TA) (Fig. 5a), as indicated by the slope of
336 1.89. The high Δ DIC points to high aerobic OM degradation and remineralization, resulting in high CO₂ production, which is
337 also indicated by seawater being supersaturated in p CO₂. High aerobic OM degradation was also previously observed in the
338 heterotrophic Wadden Sea (e.g., De Beer et al., 2005;van Beusekom et al., 1999), assuming an OM degradation and
339 remineralization occurring in the water and sediment in about equal parts (van Beusekom et al., 1999). High OM degradation
340 is indicated by the increasing C_{org}:N ratios of SPM during ebb tide (Fig. 4k, Table B1). Because we observed constant coastal
341 North Sea salinities, we rule out fresh water runoff and terrestrial signals as source for the increasing C_{org}:N ratios of SPM.
342 We assume that fresh OM is rapidly degraded in the water column, and the older OM settles on and in the sediment where the
343 degradation continues and where it is resuspended at the low prevailing water levels during ebb. Therefore, we assume that
344 the increase of SPM concentrations and their C_{org}:N ratios is an indicator for older and more refractory OM. The increase in
345 TA concentrations point to anaerobic processes, CaCO₃ dissolution, or a combination thereof as TA sources occurring in the
346 sediments.

347

348 For an upper bound estimate of sedimentary CaCO₃ dissolution as source of TA, we considered a Δ DIC: Δ TA ratio of 1:2.
349 Considering this ratio and the observed Δ TA of 51.6 μ mol TA kg⁻¹, CaCO₃ dissolution would lead to a Δ DIC of 25.8 μ mol
350 DIC kg⁻¹. The remaining 75.5 μ mol DIC kg⁻¹ (101.3 – 25.8 μ mol DIC kg⁻¹) of the observed Δ DIC in this study could then be
351 produced by OM degradation and remineralization, and would, using the theoretical expected Redfield ratio of C:N (6.6) for
352 fresh OM (Hickel, 1984), correspond to an estimated dissolved inorganic nitrogen (DIN) production of 11.4 μ mol DIN kg⁻¹.
353 However, this estimated DIN production (11.4 μ mol DIN kg⁻¹) of OM degradation and remineralization exceeds the observed
354 increase of Δ DIN (3.97 μ mol DIN L⁻¹; Table B1, sum of NO₃⁻, NO₂⁻ and NH₄⁺) during ebb tide. Based on this estimation and
355 the assumption that all DIN produced is released and thus lost, TA is probably produced by CaCO₃ dissolution and anaerobic
356 metabolic processes other than denitrification in the sediment. In addition to that, and with an N-focused perspective, the DIN
357 loss also hints to the occurrence of other processes that consume nitrogen species but have no net effect on TA, such as
358 anammox and coupled nitrification-denitrification (Hu and Cai, 2011;Middelburg et al., 2020). The suggested DIN loss can
359 be supported by considering the marine DIN:Si ratio, which is supposed to be about 1:1 (Brzezinski, 1985). We observed
360 DIN:Si ratios decreasing from 2.7 to 0.8 during ebb tide, showing that both parameter concentrations increased, whereby DIN
361 concentrations increased less than silicate concentrations. The silicate excess with respect to DIN at the end of ebb tide supports
362 the DIN loss.

363 Denitrification, the anaerobic irreversible reduction of NO_3^- to N_2 that generates 0.9 mole TA by using 1 mole NO_3^- as electron
364 acceptor (Chen and Wang, 1999) is a net TA source. Denitrification depends on the supply of nitrate, which seasonally varies
365 (van der Zee and Chou, 2005 and references therein). Generally, nitrate is depleted in summer due to high photosynthetic
366 activity and occurs in higher concentrations in winter (Kieskamp et al., 1991; Jensen et al., 1996; van der Zee and Chou, 2005).
367 This seasonality leads to denitrification rates also being lower in summer and higher in winter (Kieskamp et al., 1991; Jensen
368 et al., 1996). In previous studies, Faber et al. (2014) identified denitrification as a minor source of TA due to low denitrification
369 rates, and also Kieskamp et al. (1991) observed low denitrification rates in the Wadden Sea, with low nitrate concentrations
370 ($< 2.5 \mu\text{mol L}^{-1}$) in the water column. We observed nitrate concentrations ($< 2.17 \mu\text{mol L}^{-1}$) lower than the concentration
371 sufficient for denitrification assumed by Kieskamp et al. (1991). Therefore, we do not exclude denitrification, but suspect it as
372 a minor source of TA in the Dutch Wadden Sea at least in spring and summer due to the seasonal lack of nitrate. Thomas et
373 al. (2009) detected TA seasonality in the southern bight of the North Sea, which is also influenced by the TA generation in the
374 Wadden Sea. In addition, the estimated DIN production compared to the observed DIN not only hints to other N consuming
375 processes that have no effect on TA, but also suggests that allochthonous nitrate would be needed to fuel the TA increase by
376 denitrification.

377

378 The simultaneous increase of ammonium and TA (Fig. 4c, 4d, 5d) is important to notice, because under oxic conditions the
379 occurrence of ammonium is coupled with nitrification, a process that consumes ammonium and also TA (Chen and Wang,
380 1999). However, under anoxic conditions, such as in deeper sediment layers, ammonium cannot be reoxidized, accumulates,
381 and is washed out during ebb tide. Since we observed low nitrate concentrations and rule out terrestrial nitrate inputs here, the
382 increase in ammonium and TA implies the occurrence of other anaerobic processes of the redox system, such as sulfate and
383 iron reduction, to generate TA in the deeper, anoxic sediment layers in the Dutch Wadden Sea.

384 Sulfate reduction followed by iron reduction and the formation and burial of pyrite are net sources of TA, since TA
385 consumption by reoxidation is excluded when buried in sediments (Berner et al., 1970; Faber et al., 2014). Whether and to what
386 extent these processes contribute to TA generation in the deeper sediments of the Dutch Wadden Sea cannot be further
387 identified without the necessary data. However, sulfate reduction was also mentioned as source of TA by Thomas et al. (2009),
388 and the temporary slight appearance of noticeable sulfuric odor could be another indirect indicator for the occurrence of sulfate
389 reduction. In previous studies of tidal flats in the German Wadden Sea, Beck et al. (2008a); (2008b) observed increasing TA
390 concentrations with depth and identified sulfate reduction as the most important process for anaerobic OM remineralization in
391 pore water cores.

392

393 A strict comparison of the more northern (north of the Elbe Estuary) and the more western (Texel – Elbe Estuary) parts of the
394 Wadden Sea is difficult because the areas vary in terms of OM import and eutrophication effects (van Beusekom et al., 2019),
395 sediment composition, and extent between the barrier islands and the mainland, all of which influence the occurrence and
396 interaction of biogeochemical processes (Schwichtenberg et al., 2020). The area characteristics of the northern and western

397 Wadden Sea differ especially in terms of OM turnover being lower in the norther Wadden Sea. However, a previous study by
398 Brasse et al. (1999) identified high TA and DIC concentrations in the sediment of the North Frisian Wadden Sea and identified
399 CaCO_3 dissolution and sulfate reduction as major TA sources, which is consistent with our findings.

400 **5 Conclusion**

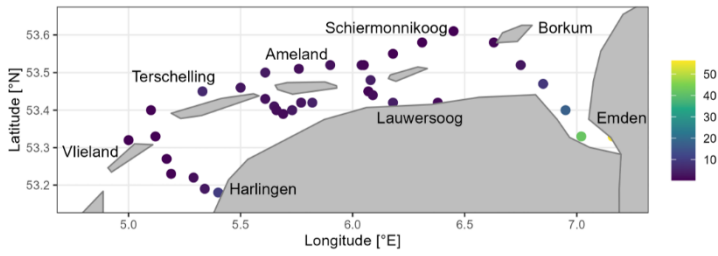
401 The Dutch Wadden Sea is a unique and highly dynamic ecosystem. We observed higher TA values in the Dutch Wadden Sea
402 than in the North Sea and identified the Dutch Wadden Sea as a TA source for the North Sea's carbonate system. Compared
403 to previous studies (Hoppema, 1990, 1993), the TA values we observed were in a similar range, with high TA values in the
404 tidal basins. Beside the need for seasonal observations, future work should also focus on regional and seasonal impacts of fresh
405 water inflows of TA on the TA status in the Dutch Wadden Sea.

406 By observing salinity and using dissolved silicate as a tracer, we excluded fresh water and river runoff as significant TA sources
407 on the tidal flats, and instead, deduced local outwash from the sediments as sources of TA. Considering various stoichiometries,
408 we suggest that CaCO_3 dissolution generates TA in the more upper oxic sediment layers, and anaerobic, metabolic processes
409 such as denitrification, sulfate and iron reduction are potential TA sources in the deeper anoxic sediment layers. However, in
410 spring and early summer, denitrification seems to play a minor role in generating TA in the sediments of the Dutch Wadden
411 Sea due to seasonality and associated limited nitrate availability.

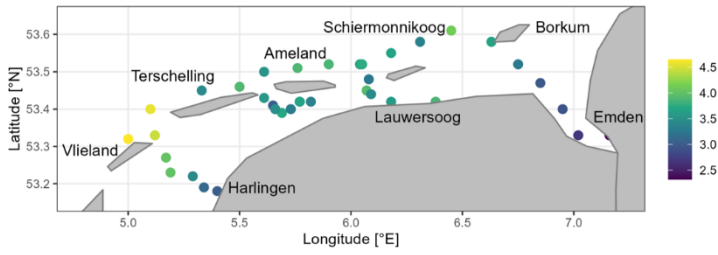
412 **6 Appendices**

413 **Appendix A**

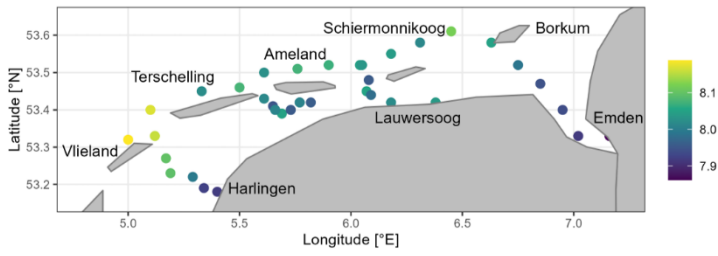
(A1a) Silicate ($\mu\text{ mol L}^{-1}$)



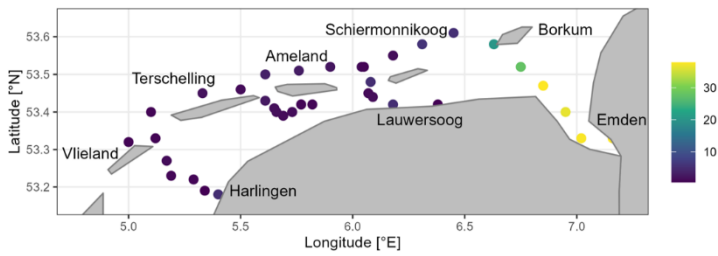
(A1b) Calcite saturation state (Ω)



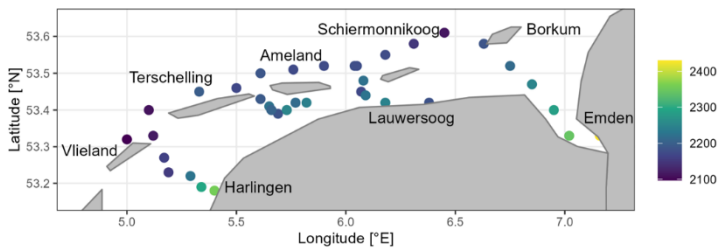
(A1c) pH



(A1d) Nitrate ($\mu\text{ mol L}^{-1}$)



(A1e) DIC ($\mu\text{ mol kg}^{-1}$)



415 **Figure A1** Spatial distribution of A1a) silicate (Si; $\mu\text{mol L}^{-1}$), A1b) calcite saturation state (Ω), A1c) pH, A1d) nitrate (NO_3^- ;
416 $\mu\text{mol L}^{-1}$), and A1e) dissolved inorganic carbon (DIC; $\mu\text{mol kg}^{-1}$) from surface water samples in May 2019.
417

418 **Appendix B**

419 **Table B1** Half tidal cycle sample parameter during ebb tide. Sample no. 545 is the first sample at high tide and sample no. 557
 420 is the last sample at low tide on 21 May 2019 (53.38°N & 5.62°E). Shown are values of temperature (Temp), salinity (Sal),
 421 total alkalinity (TA), dissolved inorganic carbon (DIC), silicate (Si), nitrate (NO₃⁻), nitrite (NO₂⁻), ammonium (NH₄⁺),
 422 phosphate (PO₄³⁻), dissolved inorganic nitrogen (DIN), the amount of carbon (C) and organic carbon (C_{org}) of SPM, the amount
 423 of nitrogen (N) of SPM, the calcite (Ca) and aragonite (Ar) saturation states, the pH, and the seawater partial pressure of CO₂
 424 (pCO₂) per sample.

Sample No.	Time [UTC]	Temp [°C]	Sal [PSU]	TA / DIC [μmol kg ⁻¹]	Si [μmol L ⁻¹]	NO ₃ ⁻ [μmol L ⁻¹]	NO ₂ ⁻ [μmol L ⁻¹]	NH ₄ ⁺ [μmol L ⁻¹]	PO ₄ ³⁻ [μmol L ⁻¹]
545	10:46	13.26	32.52	2387 / 2172	1.84	1.26	0.19	3.47	0.12
546	11:19	13.25	32.52	2385 / 2190	1.77	1.24	0.19	3.40	0.11
547	11:49	13.28	32.52	2389 / 2185	1.72	1.21	0.19	3.35	0.11
548	12:23	13.38	32.52	2391 / 2183	1.6	1.19	0.19	3.52	0.12
549	13:35	14.32	32.50	2400 / 2204	2.11	0.91	0.25	3.57	0.32
550	14:05	14.61	32.50	2400 / 2221	2.78	1.09	0.29	3.98	0.42
551	14:36	14.64	32.51	2405 / 2216	2.72	1.01	0.29	4.27	0.47
552	15:26	14.73	32.51	2411 / 2234	4.59	1.23	0.34	5.51	0.57
553	15:42	14.77	32.51	2402 / 2228	4.24	1.26	0.33	5.08	0.54
554	16:04	14.72	32.51	2419 / 2234	5.66	1.46	0.36	5.33	0.54
555	16:38	14.66	32.51	2428 / 2256	8.18	1.77	0.43	6.04	0.58
556	17:07	14.68	32.51	2433 / 2271	9.79	1.87	0.47	6.27	0.62
557	17:32	14.70	32.50	2438 / 2273	11.22	2.17	0.50	6.22	0.63
Sample No.	Time [UTC]	DIN [μmol L ⁻¹]	C / C _{org} (SPM) [μmol L ⁻¹]	N (SPM) [μmol L ⁻¹]	C _{org} :N (SPM)	SPM [mg L ⁻¹]	Ca / Ar [Ω]	pH	pCO ₂ [μatm]
545	10:46	4.93	86.8 / 65.1	8.8	7.4	12.8	3.8 / 2.4	8.07	385.1
546	11:19	4.83	72.7 / 42.4	7.4	5.8	8.7	3.5 / 2.3	8.03	430.2
547	11:49	4.76	112.4 / 93.4	9.6	9.7	15.4	3.7 / 2.3	8.05	411.4
548	12:23	4.91	108.5 / 104.6	9.9	10.5	16.8	3.7 / 2.4	8.05	404.1
549	13:35	4.73	111.1 / 97.8	8.8	11.1	13.9	3.6 / 2.3	8.01	452.3
550	14:05	5.37	233.0 / 180.3	17.7	10.2	32.2	3.3 / 2.1	7.97	507.2
551	14:36	5.56	193.2 / 174.3	14.5	12.0	29.6	3.5 / 2.2	7.99	477.9
552	15:26	7.08	248.6 / 163.5	18.4	8.9	34.3	3.3 / 2.1	7.96	520.0
553	15:42	6.67	257.6 / 199.3	18.3	10.9	41.6	3.2 / 2.1	7.95	526.4
554	16:04	7.15	324.4 / 271.1	23.2	11.7	55.0	3.4 / 2.2	7.98	496.6
555	16:38	8.24	440.4 / 345.2	29.2	11.8	75.7	3.2 / 2.1	7.95	538.0
556	17:07	8.61	430.5 / 363.3	27.9	13.0	82.4	3.1 / 2.0	7.93	576.6

557 17:32 8.90 308.9 / 199.1 21.2 9.4 48.8 3.1 / 2.0 7.93 568.4

425

426

427 **Table B2** Half tidal cycle sample parameter during high tide. Sample no. 564 is the first sample at low tide and sample no.
 428 578 is the last sample at high tide on 23 May 2019 (53.39°N & 5.63°E, 5.62°E*). Shown are values of temperature (Temp),
 429 salinity (Sal), total alkalinity (TA), dissolved inorganic carbon (DIC), silicate (Si), nitrate (NO₃⁻), nitrite (NO₂⁻), ammonium
 430 (NH₄⁺), phosphate (PO₄³⁻), dissolved inorganic nitrogen (DIN), the amount of carbon (C) and organic carbon (C_{org}) of SPM,
 431 the amount of nitrogen (N) of SPM, the calcite (Ca) and aragonite (Ar) saturation states, the pH, and the seawater partial
 432 pressure of CO₂ (pCO₂) per sample.

Sample No.	Time [UTC]	Temp [°C]	Sal [PSU]	TA / DIC [μmol kg ⁻¹]	Si [μmol L ⁻¹]	NO ₃ ⁻ [μmol L ⁻¹]	NO ₂ ⁻ [μmol L ⁻¹]	NH ₄ ⁺ [μmol L ⁻¹]	PO ₄ ³⁻ [μmol L ⁻¹]
564	05:09	14.04	32.66	2431 / 2246	8.53	1.25	0.47	3.31	0.38
565	05:32	14.02	32.68	2441 / 2287	9.14	1.26	0.45	3.08	0.37
566	06:01	13.95	32.69	2436 / 2284	8.88	1.33	0.38	2.46	0.34
567	06:33	14.16	32.69	2443 / 2284	8.68	0.95	0.37	2.37	0.33
568	07:02	14.21	32.69	2432 / 2280	6.94	0.75	0.34	2.63	0.32
569	07:31	14.15	32.55	2401 / 2223	2.12	0.98	0.27	4.12	0.33
570	08:04	14.20	32.55	2403 / 2218	2.10	1.04	0.27	3.88	0.30
571	08:35	14.27	32.55	2409 / 2228	2.15	0.92	0.25	4.18	0.32
572	09:04	14.37	32.53	2400 / 2209	1.88	1.00	0.22	3.86	0.26
573	09:34	14.16	32.52	2398 / 2200	1.70	1.03	0.21	3.51	0.21
574*	10:02	14.17	32.52	2391 / 2197	1.72	1.07	0.21	3.40	0.18
575*	10:34	14.11	32.51	2389 / 2195	1.78	1.18	0.20	3.45	0.16
576	11:04	14.21	32.50	2390 / 2187	1.76	1.12	0.19	3.29	0.14
577	11:34	14.50	32.51	2399 / 2193	1.66	1.10	0.20	3.32	0.16
578	12:03	13.96	32.51	2390 / 2187	1.75	1.41	0.19	3.72	0.11

Sample No.	Time [UTC]	DIN [μmol L ⁻¹]	C / C _{org} (SPM) [μmol L ⁻¹]	N (SPM) [μmol L ⁻¹]	C _{org} :N (SPM)	SPM [mg L ⁻¹]	Ca / Ar [Ω]	pH	pCO ₂ [μatm]
564	05:09	5.03	353.7 / 253.2	27.5	9.2	52.3	3.0 / 2.2	7.99	490.3
565	05:32	4.78	333.5 / 220.1	26.1	8.4	49.7	3.0 / 1.9	7.92	592.9
566	06:01	4.17	330.3 / 232.9	25.5	9.1	51.7	2.9 / 1.9	7.91	600.3
567	06:33	3.68	274.7 / 195.7	21.8	9.0	36.9	3.0 / 1.9	7.92	582.6
568	07:02	3.72	317.8 / 220.2	24.5	9.0	46.1	2.9 / 1.9	7.91	601.8
569	07:31	5.37	88.6 / 59.1	7.0	8.5	14.7	3.3 / 2.1	7.98	500.7
570	08:04	5.20	96.8 / 73.6	8.8	8.4	18.1	3.4 / 2.2	7.99	482.6
571	08:35	5.35	114.2 / 109.6	9.9	11.0	14.8	3.3 / 2.1	7.98	497.6

572	09:04	5.08	107.5 / 73.9	9.9	7.5	16.4	3.5 / 2.2	8.00	466.6
573	09:34	4.75	82.1 / 72.7	7.2	10.0	11.8	3.6 / 2.3	8.02	445.3
574*	10:02	4.68	85.2 / 62.9	7.2	8.7	9.9	3.5 / 2.3	8.01	450.5
575*	10:34	4.83	83.5 / 65.9	7.2	9.2	11.1	3.5 / 2.3	8.01	449.6
576	11:04	4.60	82.7 / 52.1	8.2	6.3	8.5	3.7 / 2.3	8.03	429.9
577	11:34	4.62	65.8 / 50.8	6.5	7.8	7.2	3.7 / 2.4	8.03	430.8
578	12:03	5.32	71.6 / 54.6	7.7	7.1	7.7	3.7 / 2.3	8.04	425.3

433

434

435 **Table B3** Transect parameter of cruise LP20190515 on RV *Ludwig Prandt* in the Dutch Wadden Sea in May 2019. Shown
436 are values of latitude (Lat), longitude (Lon), temperature (Temp), salinity (Sal), total alkalinity (TA), dissolved inorganic
437 carbon (DIC), silicate (Si), nitrate (NO₃⁻), the calcite (Ca) and aragonite (Ar) saturation states, and pH per sample. Our salinity
438 and temperature data were complemented by data of three Rijkswaterstaat stations, which were close to our stations. There,
439 Dantziggat* (53°24'4.093", 5°43'37.132") showed temperatures of 11.4 and 14.9 °C and salinities of 31.9 and 31.2 on 10 and
440 27 May 2019, respectively, Terschelling 10** (53°27'37.318", 5°5'58.129") showed temperatures of 11.4 and 12.9 °C and
441 salinities of 32.8 and 33.4 on 15 and 28 May 2019, respectively, and Vliestroom*** (53°18'48.054", 5°9'35.655") showed a
442 temperature of 11.8 °C and a salinity of 31.1 on 14 May 2019.

Sample No.	Time [UTC]	Day May	Lat. [°N]	Lon. [°E]	Temp [°C]	Sal [PSU]	TA / DIC [μmol kg ⁻¹]	Si / NO ₃ ⁻ [μmol L ⁻¹]	Ca / Ar [Ω]	pH
535	07:56	20	53.18	5.4	14.72	30.24	2507 / 2357	10.00 / 5.10	3.0 / 1.9	7.92
536	08:26	20	53.19	5.34	14.81	32.51	2458 / 2296	3.45 / 0.46	3.1 / 2.0	7.92
537	08:53	20	53.22	5.29	14.05	32.38	2413 / 2227	1.92 / 0.85	3.4 / 2.2	8.00
538	09:28	20	53.23	5.19	13.36	32.65	2381 / 2153	0.52 / 1.02	4.0 / 2.6	8.10
539	09:53	20	53.27	5.17	13.17	32.65	2389 / 2161	0.45 / 1.37	4.0 / 2.6	8.10
540***	10:36	20	53.33	5.12	12.77	32.97	2375 / 2118	0.32 / 0.84	4.4 / 2.8	8.16
541	11:03	20	53.32	5.0	12.41	33.25	2368 / 2097	0.34 / 0.77	4.6 / 3.0	8.19
542**	11:49	20	53.4	5.1	12.93	32.92	2374 / 2109	0.44 / 0.81	4.6 / 2.9	8.17
543	12:49	20	53.45	5.33	12.95	32.45	2385 / 2196	6.25 / 1.85	3.4 / 2.2	8.02
544	13:31	20	53.46	5.5	13.55	32.51	2388 / 2169	3.02 / 1.30	3.9 / 2.5	8.08
558	11:33	22	53.41	5.65	13.31	32.51	2384 / 2224	2.57 / 1.56	3.0 / 1.9	7.95
559	12:04	22	53.4	5.66	13.45	32.51	2393 / 2195	1.58 / 1.41	3.6 / 2.3	8.03
560	12:40	22	53.39	5.69	13.67	32.52	2391 / 2183	1.52 / 1.33	3.7 / 2.4	8.05
561	13:09	22	53.4	5.73	14.23	32.48	2418 / 2242	2.04 / 1.04	3.3 / 2.1	7.97
562	13:32	22	53.42	5.77	14.71	32.51	2417 / 2237	3.23 / 1.04	3.3 / 2.1	7.97

563*	13:56	22	53.42	5.82	15.33	32.45	2421 / 2242	4.68 / 0.86	3.3 / 2.1	7.96
579	09:05	24	53.42	5.77	15.26	32.65	2417 / 2215	2.71 / 0.86	3.7 / 2.4	8.01
580	09:31	24	53.4	5.73	14.99	32.66	2426 / 2249	3.52 / 1.46	3.3 / 2.1	7.95
581	10:01	24	53.4	5.66	13.87	32.58	2396 / 2205	1.69 / 1.60	3.5 / 2.2	8.01
582	10:25	24	53.43	5.61	14.36	32.51	2389 / 2193	2.23 / 2.52	3.6 / 2.3	8.02
583	10:59	24	53.5	5.61	13.48	32.58	2382 / 2187	3.69 / 3.41	3.5 / 2.2	8.03
584	11:31	24	53.51	5.76	13.50	32.59	2390 / 2172	1.93 / 2.96	3.9 / 2.5	8.07
585	12:00	24	53.52	5.9	13.65	32.59	2390 / 2173	2.34 / 2.23	3.9 / 2.5	8.07
586	12:30	24	53.52	6.04	13.50	32.48	2384 / 2179	2.00 / 1.53	3.7 / 2.3	8.05
587	13:02	24	53.45	6.07	15.13	32.40	2389 / 2169	0.70 / 1.19	3.9 / 2.5	8.05
588	13:31	24	53.42	6.38	15.63	31.96	2396 / 2182	1.33 / 0.62	3.9 / 2.5	8.04
589	07:20	25	53.42	6.18	15.73	28.31	2430 / 2245	4.16 / 5.13	3.6 / 2.3	8.02
590	07:52	25	53.44	6.09	15.80	30.90	2407 / 2225	1.58 / 1.39	3.4 / 2.2	7.98
591	08:21	25	53.48	6.08	15.34	31.82	2395 / 2222	4.16 / 5.09	3.3 / 2.1	7.96
592	08:51	25	53.52	6.05	14.80	32.41	2386 / 2178	0.71 / 0.67	3.8 / 2.4	8.04
593	09:22	25	53.55	6.18	13.96	32.30	2379 / 2175	0.36 / 1.52	3.7 / 2.3	8.04
594	09:53	25	53.58	6.31	13.43	32.14	2332 / 2148	0.34 / 5.75	3.3 / 2.1	8.01
595	10:24	25	53.61	6.45	13.47	32.10	2347 / 2113	0.26 / 5.19	4.1 / 2.6	8.12
596	11:05	25	53.58	6.63	14.50	29.99	2381 / 2184	0.78 / 20.25	3.7 / 2.3	8.05
597	11:33	25	53.52	6.75	14.94	29.17	2383 / 2214	3.04 / 27.84	3.3 / 2.1	7.99
598	12:00	25	53.47	6.85	15.28	27.82	2395 / 2249	8.90 / 37.93	3.0 / 1.9	7.94
599	12:30	25	53.4	6.95	15.46	26.39	2423 / 2284	17.63 / 36.54	2.9 / 1.8	7.94
600	12:59	25	53.33	7.02	15.76	23.01	2460 / 2343	41.93 / 37.68	2.7 / 1.7	7.92
601	13:29	25	53.33	7.16	15.96	20.25	2517 / 2430	56.32 / 37.94	2.3 / 1.4	7.86

443

444 **Data availability**

445 The data of this study are presented in the appendices of this article.

446 **Author Contributions**

447 MN wrote the manuscript, did the carbon sampling and sample measurement, analyzed and evaluated the data, and led the
448 study. JvB led the research cruise. JvB and HT contributed with editorial and scientific recommendations. MN prepared the
449 manuscript with contribution from all co-authors.

450 **Competing interests**

451 The contact author has declared that none of the authors has any competing interests.

452 **Acknowledgement**

453 We thank the crew from RV *Ludwig Prandtl* for their support during the cruise. We thank Leon Schmidt for the nutrient
454 sampling and measurements, Marc Metzke for the C/N measurements, and Yoana Voynova and her department for the
455 FerryBox preparation. We further thank the Editor and two anonymous reviewers for their constructive comments, which
456 greatly improved this manuscript.

457 **Financial support**

458 This research has been funded by the German Academic Exchange Service (DAAD, project: MOPGA-GRI, grant no.
459 57429828), which received funds from the German Federal Ministry of Education and Research (BMBF).

460 **References**

- 461 Abril, G., and Frankignoulle, M.: Nitrogen–alkalinity interactions in the highly polluted Scheldt basin (Belgium), *Water Research*, 35, 844-
462 850, [https://doi.org/10.1016/S0043-1354\(00\)00310-9](https://doi.org/10.1016/S0043-1354(00)00310-9), 2001.
- 463 Beck, M., Dellwig, O., Holstein, J. M., Grunwald, M., Liebezeit, G., Schnetger, B., and Brumsack, H.-J.: Sulphate, dissolved organic carbon,
464 nutrients and terminal metabolic products in deep pore waters of an intertidal flat, *Biogeochemistry*, 89, 221-238,
465 <https://doi.org/10.1007/s10533-008-9215-6>, 2008a.
- 466 Beck, M., Dellwig, O., Liebezeit, G., Schnetger, B., and Brumsack, H.-J.: Spatial and seasonal variations of sulphate, dissolved organic
467 carbon, and nutrients in deep pore waters of intertidal flat sediments, *Estuarine, Coastal and Shelf Science*, 79, 307-316,
468 <https://doi.org/10.1016/j.ecss.2008.04.007>, 2008b.
- 469 Berner, R. A., Scott, M. R., and Thomlinson, C.: Carbonate alkalinity in the pore waters of anoxic marine sediments 1, *Limnology and*
470 *Oceanography*, 15, 544-549, <https://doi.org/10.4319/lo.1970.15.4.0544>, 1970.
- 471 Berner, R. A., Lasaga, A. C., and Garrels, R. M.: Carbonate-silicate geochemical cycle and its effect on atmospheric carbon dioxide over
472 the past 100 million years, *Am. J. Sci. (United States)*, 283, doi:10.2475/ajs.283.7.641., 1983.
- 473 Billerbeck, M., Werner, U., Polerecky, L., Walpersdorf, E., DeBeer, D., and Huettel, M.: Surficial and deep pore water circulation governs
474 spatial and temporal scales of nutrient recycling in intertidal sand flat sediment, *Marine Ecology Progress Series*, 326, 61-76, 2006.
- 475 Borges, A. V., Delille, B., and Frankignoulle, M.: Budgeting sinks and sources of CO₂ in the coastal ocean: Diversity of ecosystems counts,
476 *Geophysical research letters*, 32, doi.org/10.1029/2005GL023053, 2005.
- 477 Bozec, Y., Thomas, H., Elkalay, K., and de Baar, H. J.: The continental shelf pump for CO₂ in the North Sea—evidence from summer
478 observation, *Marine Chemistry*, 93, 131-147, <https://doi.org/10.1016/j.marchem.2004.07.006>, 2005.

479 Brasse, S., Reimer, A., Seifert, R., and Michaelis, W.: The influence of intertidal mudflats on the dissolved inorganic carbon and total
480 alkalinity distribution in the German Bight, southeastern North Sea, *Journal of Sea Research*, 42, 93-103, 1999.

481 Brenner, H., Braeckman, U., Le Guitton, M., and Meysman, F. J.: The impact of sedimentary alkalinity release on the water column CO₂
482 system in the North Sea, *Biogeosciences*, 13, 841-863, <https://doi.org/10.5194/bg-13-841-2016>, 2016.

483 Brewer, P. G., and Goldman, J. C.: Alkalinity changes generated by phytoplankton growth, *Limnology and Oceanography*, 21, 108-117,
484 <https://doi.org/10.4319/lo.1976.21.1.0108>, 1976.

485 Brzezinski, M. A.: The Si: C: N ratio of marine diatoms: interspecific variability and the effect of some environmental variables, *Journal of*
486 *Phycology*, 21, 347-357, <https://doi.org/10.1111/j.0022-3646.1985.00347.x>, 1985.

487 Burchard, H., Flöser, G., Staneva, J. V., Badewien, T. H., and Riethmüller, R.: Impact of density gradients on net sediment transport into
488 the Wadden Sea, *Journal of Physical Oceanography*, 38, 566-587, 2008.

489 Burt, W., Thomas, H., Hagens, M., Pätsch, J., Clargo, N., Salt, L., Winde, V., and Böttcher, M.: Carbon sources in the North Sea evaluated
490 by means of radium and stable carbon isotope tracers, *Limnology and Oceanography*, 61, 666-683, <https://doi.org/10.1002/lno.10243>, 2016.

491 Carter, B. R., Toggweiler, J., Key, R. M., and Sarmiento, J. L.: Processes determining the marine alkalinity and calcium carbonate saturation
492 state distributions, *Biogeosciences*, 11, 7349-7362, <https://doi.org/10.5194/bg-11-7349-2014>, 2014.

493 Charalampopoulou, A., Poulton, A. J., Tyrrell, T., and Lucas, M. I.: Irradiance and pH affect coccolithophore community composition on a
494 transect between the North Sea and the Arctic Ocean, *Marine Ecology Progress Series*, 431, 25-43, <https://doi.org/10.3354/meps09140>,
495 2011.

496 Chen, C. T. A., and Wang, S. L.: Carbon, alkalinity and nutrient budgets on the East China Sea continental shelf, *Journal of Geophysical*
497 *Research: Oceans*, 104, 20675-20686, <https://doi.org/10.1029/1999JC900055>, 1999.

498 Crutzen, P.: Geology of mankind, *Nature*, 415, <https://doi.org/10.1038/415023a>, 2002.

499 De Beer, D., Wenzhöfer, F., Ferdelman, T. G., Boehme, S. E., Huettel, M., van Beusekom, J. E., Böttcher, M. E., Musat, N., and Dubilier,
500 N.: Transport and mineralization rates in North Sea sandy intertidal sediments, Sylt-Rømø basin, Wadden Sea, *Limnology and*
501 *Oceanography*, 50, 113-127, 2005.

502 De Jonge, V., Essink, K., and Boddeke, R.: The Dutch Wadden Sea: a changed ecosystem, *Hydrobiologia*, 265, 45-71,
503 <https://doi.org/10.1007/BF00007262>, 1993.

504 Dickson, A., and Millero, F. J.: A comparison of the equilibrium constants for the dissociation of carbonic acid in seawater media, *Deep Sea*
505 *Research Part A. Oceanographic Research Papers*, 34, 1733-1743, [https://doi.org/10.1016/0198-0149\(87\)90021-5](https://doi.org/10.1016/0198-0149(87)90021-5), 1987.

506 Dickson, A. G.: An exact definition of total alkalinity and a procedure for the estimation of alkalinity and total inorganic carbon from titration
507 data, *Deep Sea Research Part A. Oceanographic Research Papers*, 28, 609-623, [https://doi.org/10.1016/0198-0149\(81\)90121-7](https://doi.org/10.1016/0198-0149(81)90121-7), 1981.

508 Duran-Matute, M., Gerkema, T., De Boer, G., Nauw, J., and Gräwe, U.: Residual circulation and freshwater transport in the Dutch Wadden
509 Sea: a numerical modelling study, *Ocean Science*, 10, 611-632, 2014.

510 Elias, E. P., Van der Spek, A. J., Wang, Z. B., and De Ronde, J.: Morphodynamic development and sediment budget of the Dutch Wadden
511 Sea over the last century, *Netherlands Journal of Geosciences*, 91, 293-310, <https://doi.org/10.1017/S0016774600000457>, 2012.

512 Faber, P. A., Evrard, V., Woodland, R. J., Cartwright, I. C., and Cook, P. L.: Pore-water exchange driven by tidal pumping causes alkalinity
513 export in two intertidal inlets, *Limnology and Oceanography*, 59, 1749-1763, <https://doi.org/10.4319/lo.2014.59.5.1749>, 2014.

514 Friedlingstein, P., O'sullivan, M., Jones, M. W., Andrew, R. M., Gregor, L., Hauck, J., Le Quééré, C., Luijckx, I. T., Olsen, A., and Peters, G.
515 P.: Global carbon budget 2022, *Earth System Science Data*, 14, 4811-4900, 2022.

516 Glavovic, B., Limburg, K., Liu, K., Emeis, K., Thomas, H., Kremer, H., Avril, B., Zhang, J., Mulholland, M., and Glaser, M.: Living on the
517 Margin in the Anthropocene: engagement arenas for sustainability research and action at the ocean-land interface, *Current Opinion in*
518 *Environmental Sustainability*, 14, 232-238, <https://doi.org/10.1016/j.cosust.2015.06.003>, 2015.

519 Grasshoff, K., Kremling, K., and Ehrhardt, M.: *Methods of seawater analysis*, John Wiley & Sons, 2009.

520 Hansen, H., and Koroleff, F.: Determination of nutrients. *Methods of Seawater Analysis: Third, Completely Revised and Extended Edition*.
521 Grasshoff, K., Kremling, K., and Ehrhardt, M. (Eds.), Weinheim, Germany: Wiley-VCH Verlag GmbH, 2007.

522 Hickel, W.: *Seston in the Wadden Sea of Sylt (German Bight, North Sea)*, Netherlands Institute for Sea Research - Publication Series, 10,
523 113-131, 1984.

524 Hoppema, J.: The distribution and seasonal variation of alkalinity in the southern bight of the North Sea and in the western Wadden Sea,
525 *Netherlands journal of sea research*, 26, 11-23, [https://doi.org/10.1016/0077-7579\(90\)90053-J](https://doi.org/10.1016/0077-7579(90)90053-J), 1990.

526 Hoppema, J.: The oxygen budget of the western Wadden Sea, *The Netherlands, Estuarine, Coastal and Shelf Science*, 32, 483-502,
527 [https://doi.org/10.1016/0272-7714\(91\)90036-B](https://doi.org/10.1016/0272-7714(91)90036-B), 1991.

528 Hoppema, J.: Carbon dioxide and oxygen disequilibrium in a tidal basin (Dutch Wadden Sea), *Netherlands journal of sea research*, 31, 221-
529 229, [https://doi.org/10.1016/0077-7579\(93\)90023-L](https://doi.org/10.1016/0077-7579(93)90023-L), 1993.

530 Hu, X., and Cai, W. J.: An assessment of ocean margin anaerobic processes on oceanic alkalinity budget, *Global Biogeochemical Cycles*,
531 25, doi.org/10.1029/2010GB003859, 2011.

532 Huettel, M., Røy, H., Precht, E., and Ehrenhauss, S.: Hydrodynamical impact on biogeochemical processes in aquatic sediments, *The*
533 *Interactions between Sediments and Water: Proceedings of the 9th International Symposium on the Interactions between Sediments and*
534 *Water*, held 5-10 May 2002 in Banff, Alberta, Canada, 2003, 231-236,

535 Jahnke, R. A., Craven, D. B., and Gaillard, J.-F.: The influence of organic matter diagenesis on CaCO₃ dissolution at the deep-sea floor,
536 *Geochimica et Cosmochimica Acta*, 58, 2799-2809, 1994.

537 Jensen, K., Jensen, M., and Kristensen, E.: Nitrification and denitrification in Wadden Sea sediments (Königshafen, Island of Sylt, Germany)
538 as measured by nitrogen isotope pairing and isotope dilution, *Aquatic Microbial Ecology*, 11, 181-191, doi:10.3354/ame011181, 1996.

539 Keith, D. W., Ha-Duong, M., and Stolaroff, J. K.: Climate strategy with CO₂ capture from the air, *Climatic Change*, 74, 17-45,
540 <https://doi.org/10.1007/s10584-005-9026-x>, 2006.

541 Kérouel, R., and Aminot, A.: Fluorometric determination of ammonia in sea and estuarine waters by direct segmented flow analysis, *Marine*
542 *Chemistry*, 57, 265-275, [https://doi.org/10.1016/S0304-4203\(97\)00040-6](https://doi.org/10.1016/S0304-4203(97)00040-6), 1997.

543 Kieskamp, W. M., Lohse, L., Epping, E., and Helder, W.: Seasonal variation in denitrification rates and nitrous oxide fluxes in intertidal
544 sediments of the western Wadden Sea, *Marine ecology progress series*. Oldendorf, 72, 145-151, 1991.

545 Lewis, E., and Wallace, D.: Program developed for CO₂ system calculations, *Environmental System Science Data Infrastructure for a Virtual*
546 *Ecosystem*, 1998.

547 Louters, T., and Gerritsen, F.: The Riddle of the Sands: A Tidal System Vs Answer to a Rising Sea Level, report RIKZ-94.040 (isbn 90-369-
548 0084-0), 1994.

549 Matthews, H. D., and Caldeira, K.: Stabilizing climate requires near-zero emissions, *Geophysical research letters*, 35,
550 <https://doi.org/10.1029/2007GL032388>, 2008.

551 Mehrbach, C., Culberson, C., Hawley, J., and Pytkowicz, R.: Measurement of the apparent dissociation constants of carbonic acid in seawater
552 at atmospheric pressure, *Limnology and oceanography*, 18, 897-907, <https://doi.org/10.4319/lo.1973.18.6.0897>, 1973.

553 Meybeck, M.: Global chemical weathering of surficial rocks estimated from river dissolved loads, *American journal of science*, 287, 401-
554 428, 10.2475/ajs.287.5.401, 1987.

555 Middelburg, J. J., Soetaert, K., and Hagens, M.: Ocean alkalinity, buffering and biogeochemical processes, *Reviews of Geophysics*, 58,
556 e2019RG000681, <https://doi.org/10.1029/2019RG000681>, 2020.

557 Millero, F. J., Byrne, R. H., Wanninkhof, R., Feely, R., Clayton, T., Murphy, P., and Lamb, M. F.: The internal consistency of CO₂
558 measurements in the equatorial Pacific, *Marine Chemistry*, 44, 269-280, 1993.

559 Norbistrath, M., Pätsch, J., Dähnke, K., Sanders, T., Schulz, G., van Beusekom, J. E., and Thomas, H.: Metabolic alkalinity release from
560 large port facilities (Hamburg, Germany) and impact on coastal carbon storage, *Biogeosciences*, 19, 5151-5165, <https://doi.org/10.5194/bg-19-5151-2022>, 2022.

562 Norbistrath, M., Neumann, A., Dähnke, K., Sanders, T., Schöl, A., van Beusekom, J. E., and Thomas, H.: Alkalinity and nitrate dynamics
563 reveal dominance of anammox in a hyper-turbid estuary, *Biogeosciences*, 20, 4307-4321, <https://doi.org/10.5194/bg-20-4307-2023>, 2023.

564 Orr, J. C., Epitalon, J.-M., Dickson, A. G., and Gattuso, J.-P.: Routine uncertainty propagation for the marine carbon dioxide system, *Marine*
565 *Chemistry*, 207, 84-107, 2018.

566 Pätsch, J.: Daily Loads of Nutrients, Total Alkalinity, Dissolved Inorganic Carbon and Dissolved Organic Carbon of the European
567 Continental Rivers for the Years 1977 – 2022. 2024.

568 Petersen, W., Schroeder, F., and Bockelmann, F.-D.: FerryBox-Application of continuous water quality observations along transects in the
569 North Sea, *Ocean Dynamics*, 61, 1541-1554, <https://doi.org/10.1007/s10236-011-0445-0>, 2011.

570 Postma, H.: Hydrography of the Dutch Wadden sea, *Arch. Neerl. Zool*, 10, 405-511, 1954.

571 Renforth, P., and Henderson, G.: Assessing ocean alkalinity for carbon sequestration, *Reviews of Geophysics*, 55, 636-674,
572 <https://doi.org/10.1002/2016RG000533>, 2017.

573 Ridderinkhof, H., Zimmerman, J., and Philippart, M.: Tidal exchange between the North Sea and Dutch Wadden Sea and mixing time scales
574 of the tidal basins, *Netherlands Journal of Sea Research*, 25, 331-350, [https://doi.org/10.1016/0077-7579\(90\)90042-F](https://doi.org/10.1016/0077-7579(90)90042-F), 1990.

575 Røy, H., Lee, J. S., Jansen, S., and de Beer, D.: Tide-driven deep pore-water flow in intertidal sand flats, *Limnology and oceanography*, 53,
576 1521-1530, <https://doi.org/10.4319/lo.2008.53.4.1521>, 2008.

577 Rutgers van der Loeff, M.: Transport van reactief silikaat uit Waddenzee sediment naar het bovenstaande water, NIOZ-rapport, 1974.

578 Sabine, C. L., Feely, R. A., Gruber, N., Key, R. M., Lee, K., Bullister, J. L., Wanninkhof, R., Wong, C., Wallace, D. W., and Tilbrook, B.:
579 The oceanic sink for anthropogenic CO₂, *science*, 305, 367-371, DOI: 10.1126/science.1097403, 2004.

580 Santos, I. R., Chen, X., Lecher, A. L., Sawyer, A. H., Moosdorf, N., Rodellas, V., Tamborski, J., Cho, H.-M., Dimova, N., and Sugimoto,
581 R.: Submarine groundwater discharge impacts on coastal nutrient biogeochemistry, *Nature Reviews Earth & Environment*, 2, 307-323,
582 <https://doi.org/10.1038/s43017-021-00152-0>, 2021.

583 Schwichtenberg, F., Callies, U., and van Beusekom, J. E.: Residence times in shallow waters help explain regional differences in Wadden
584 Sea eutrophication, *Geo-Marine Letters*, 37, 171-177, <https://doi.org/10.1007/s00367-016-0482-2>, 2017.

585 Schwichtenberg, F., Pätsch, J., Böttcher, M. E., Thomas, H., Winde, V., and Emeis, K.-C.: The impact of intertidal areas on the carbonate
586 system of the southern North Sea, *Biogeosciences*, 17, 4223-4245, <https://doi.org/10.5194/bg-17-4223-2020>, 2020.

587 Shadwick, E., Thomas, H., Gratton, Y., Leong, D., Moore, S., Papakyriakou, T., and Prowe, A.: Export of Pacific carbon through the Arctic
588 Archipelago to the North Atlantic, *Continental Shelf Research*, 31, 806-816, <https://doi.org/10.1016/j.csr.2011.01.014>, 2011.

589 Suchet, P. A., and Probst, J.-L.: Modelling of atmospheric CO₂ consumption by chemical weathering of rocks: application to the Garonne,
590 Congo and Amazon basins, *Chemical Geology*, 107, 205-210, DOI:10.1016/0009-2541(93)90174-H, 1993.

591 Thomas, H., Bozec, Y., Elkalay, K., and De Baar, H. J.: Enhanced open ocean storage of CO₂ from shelf sea pumping, *Science*, 304, 1005-
592 1008, DOI: 10.1126/science.1095491, 2004.

593 Thomas, H., Schiettecatte, L.-S., Suykens, K., Koné, Y., Shadwick, E., Prowe, A. F., Bozec, Y., de Baar, H. J., and Borges, A.: Enhanced
594 ocean carbon storage from anaerobic alkalinity generation in coastal sediments, *Biogeosciences*, 6, 267-274, [https://doi.org/10.5194/bg-6-
595 267-2009](https://doi.org/10.5194/bg-6-267-2009), 2009.

596 van Bennekom, A., Krijgsman-van Hartingsveld, E., van der Veer, G., and van Voorst, H.: The seasonal cycles of reactive silicate and
597 suspended diatoms in the Dutch Wadden Sea, *Netherlands Journal of Sea Research*, 8, 174-207, [https://doi.org/10.1016/0077-
598 7579\(74\)90016-7](https://doi.org/10.1016/0077-7579(74)90016-7), 1974.

599 van Beusekom, J., Brockmann, U., Hesse, K.-J., Hickel, W., Poremba, K., and Tillmann, U.: The importance of sediments in the
600 transformation and turnover of nutrients and organic matter in the Wadden Sea and German Bight, *Deutsche Hydrografische Zeitschrift*, 51,
601 245-266, 10.1007/BF02764176, 1999.

602 van Beusekom, J., and De Jonge, V.: Long-term changes in Wadden Sea nutrient cycles: importance of organic matter import from the North
603 Sea, in: *Nutrients and Eutrophication in Estuaries and Coastal Waters*, Springer, 185-194, 2002.

604 van Beusekom, J. E., Buschbaum, C., and Reise, K.: Wadden Sea tidal basins and the mediating role of the North Sea in ecological processes:
605 scaling up of management?, *Ocean & coastal management*, 68, 69-78, <https://doi.org/10.1016/j.ocecoaman.2012.05.002>, 2012.

606 van Beusekom, J. E., Carstensen, J., Dolch, T., Grage, A., Hofmeister, R., Lenhart, H., Kerimoglu, O., Kolbe, K., Pätsch, J., and Rick, J.:
607 Wadden Sea Eutrophication: long-term trends and regional differences, *Frontiers in Marine Science*, 6, 370,
608 doi.org/10.3389/fmars.2019.00370, 2019.

609 van der Zee, C., and Chou, L.: Seasonal cycling of phosphorus in the Southern Bight of the North Sea, *Biogeosciences*, 2, 27-42,
610 <https://doi.org/10.5194/bg-2-27-2005>, 2005.

611 van Raaphorst, W., and van der Veer, H. W.: The phosphorus budget of the Marsdiep tidal basin (Dutch Wadden Sea) in the period 1950–
612 1985: importance of the exchange with the North Sea, in: *North Sea—Estuaries Interactions*, Springer, 21-38, 1990.

613 Voynova, Y. G., Petersen, W., Gehrung, M., Aßmann, S., and King, A. L.: Intertidal regions changing coastal alkalinity: The Wadden Sea-
614 North Sea tidally coupled bioreactor, *Limnology and Oceanography*, 64, 1135-1149, 2019.

615 Wang, Z. A., Kroeger, K. D., Ganju, N. K., Gonneea, M. E., and Chu, S. N.: Intertidal salt marshes as an important source of inorganic
616 carbon to the coastal ocean, *Limnology and Oceanography*, 61, 1916-1931, 2016.

617 Waska, H., and Kim, G.: Submarine groundwater discharge (SGD) as a main nutrient source for benthic and water-column primary
618 production in a large intertidal environment of the Yellow Sea, *Journal of Sea Research*, 65, 103-113,
619 <https://doi.org/10.1016/j.seares.2010.08.001>, 2011.

620 Wolf-Gladrow, D. A., Zeebe, R. E., Klaas, C., Körtzinger, A., and Dickson, A. G.: Total alkalinity: The explicit conservative expression and
621 its application to biogeochemical processes, *Marine Chemistry*, 106, 287-300, <https://doi.org/10.1016/j.marchem.2007.01.006>, 2007.

622 Wu, Z., Zhou, H., Zhang, S., and Liu, Y.: Using ²²²Rn to estimate submarine groundwater discharge (SGD) and the associated nutrient fluxes
623 into Xiangshan Bay, East China Sea, *Marine pollution bulletin*, 73, 183-191, <https://doi.org/10.1016/j.marpolbul.2013.05.024>, 2013.

624 Zalasiewicz, J., Williams, M., Steffen, W., and Crutzen, P.: *The new world of the Anthropocene*. ACS Publications, 2010.

625 Zhang, C., Shi, T., Liu, J., He, Z., Thomas, H., Dong, H., Rinkevich, B., Wang, Y., Hyun, J.-H., and Weinbauer, M.: Eco-engineering
626 approaches for ocean negative carbon emission, *Science Bulletin*, 67, 2564-2573, <https://doi.org/10.1016/j.scib.2022.11.016>, 2022.

627